Figure 5. The anti-HCV activity of N-89 or N-251 was canceled by addition of VE. Effect of VE on the anti-HCV activity of N-89 (A), N-251 (C), Artemisinin (E), CsA, or IFN-α at the expected EC_{90}. ORL8 cells were treated with control medium (−), N-89, CsA, or IFN-α in either the absence or presence of VE for 72 hrs. After treatment, an RL assay of harvested ORL8 cell samples was performed. (B, D, and F) The ratio of RL activity in the presence of VE to the RL activity in the absence of VE. The above ratio was calculated from the data of (A, C, and E). The horizontal line indicates the promoting effect of VE alone on HCV-RNA replication as a baseline. (G) Western blot analysis was performed as described in Fig. 1B.
doi:10.1371/journal.pone.0072519.g005

cell counting after trypan blue dye treatment revealed that approximately 30% of the cells were viable (data not shown). These results suggest that the inhibitory effect of N-89 or N-251 on HCV-RNA replication may depend on genotype 1b or not work for only JFH-1 strain.

OR6 and ORL8 Cells were Cured by Treatment with only N-89

To date, IFN-α alone or IFN-γ alone has generally been used to prepare cured cells from the cells harboring HCV-RNA [36]. Since we observed strong anti-HCV activity (>99% suppression) at 8 μM of N-89 in OR6 cells or 1 μM of N-89 in ORL8 cells without a decrease in cell viability (Fig. 1B), we expected that these cells might be cured only by treatment with N-89. Accordingly, OR6 and ORL8 cells were treated with 8 μM and 1 μM of N-89, respectively, in the absence of G418. The treatment was continued for 3 weeks with the addition of N-89 at 4-day intervals. All of the treated cells were dead when cultured in the presence of G418 for an additional two weeks, whereas the treated cells proliferated efficiently in the absence of G418 (Fig. 3), suggesting that OR6 and ORL8 cells are cured by monotherapy with N-89. This suggestion was confirmed by Western blot analysis (Fig. 3). These results indicate that N-89 is a strong anti-HCV reagent, which can be used to prepare cured cells by treatment at low concentration.

Comparative Time Course Assay of the Anti-HCV Activities of N-89 and IFN-α

We next performed a time course assay (2 to 72 hrs after treatment) in the case of ORL8 cells treated with N-89 (0.1 μM or 1 μM) or IFN-α (1 IU/ml; corresponding to approximately EC_{80}). ORL8 cells treated with IFN-α (1 IU/ml) and N-89 (1 μM) had almost the same anti-HCV kinetics over the first 24 hrs after treatment (upper panel of Fig. 4); however, within the first 12 hrs after treatment N-89-treated ORL8 cells had more rapid anti-HCV kinetics than did the IFN-α-treated cells (lower panel of Fig. 4). N-89 at concentrations of 0.1 μM and 1 μM led to

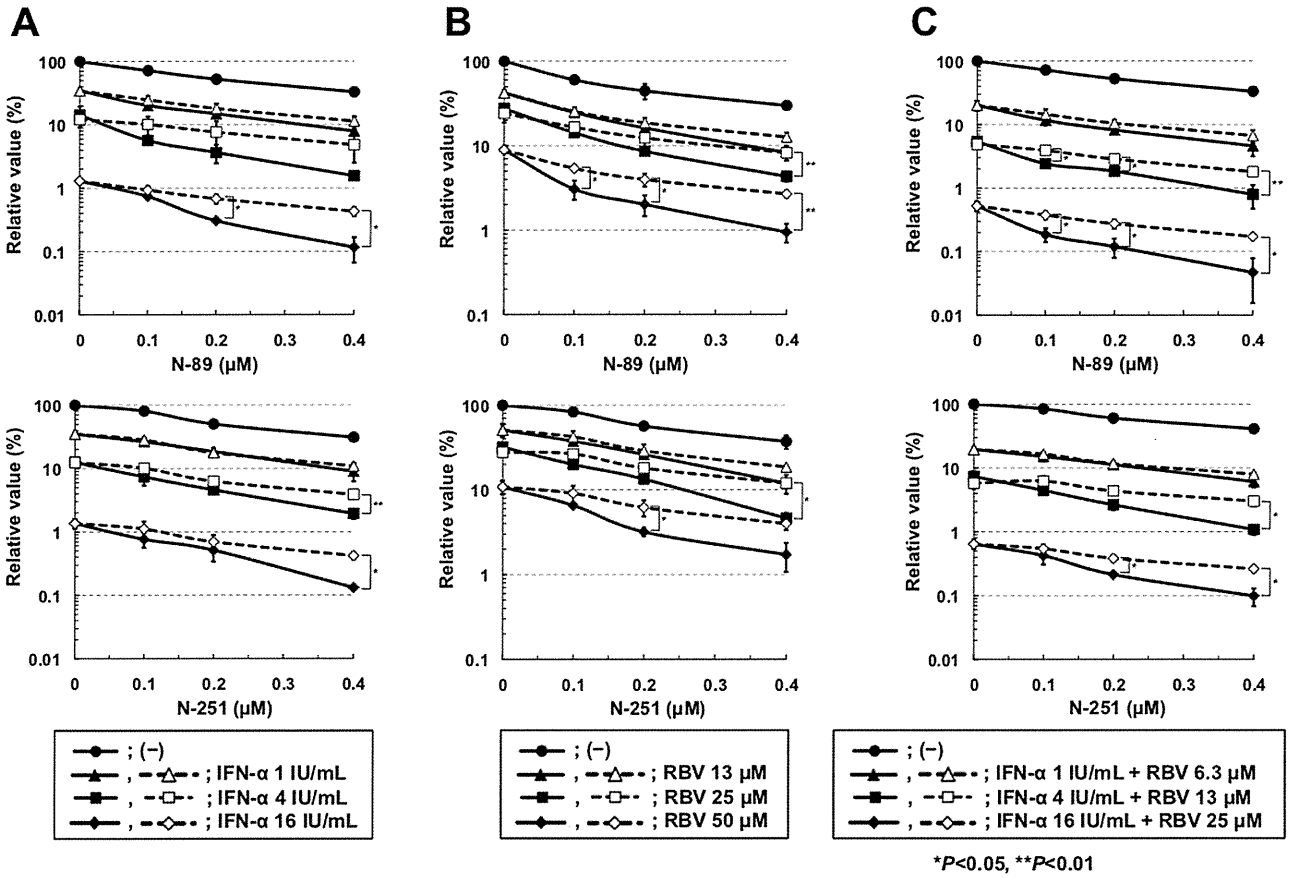

Figure 6. Synergistic anti-HCV effects of N-89 or N-251 in combination with IFN-α and/or RBV on HCV-RNA replication in ORL8 cells. Open symbols in the broken lines show the values expected as an additive anti-HCV effect and closed symbols in the solid lines show the values obtained by the ORL8 assay. ORL8 cells were treated with N-89 (upper panel) or N-251 (lower panel) in combination with IFN-α (A), RBV (B), or IFN-α and RBV (C) for 72 hrs and subjected to RL assay.
doi:10.1371/journal.pone.0072519.g006

significantly decreased RL activity at 9 hrs and 6 hrs, respectively, after treatment, whereas a decrease of RL activity in the cells treated with 1 IU/ml of IFN-α began to be seen at 12 hrs after treatment (lower panel of Fig. 4). These results suggest that the action of N-89, and probably also that of N-251, is faster than that of IFN-α, and the anti-HCV mechanism of N-89 is different from that of IFN-α.

Synergistic Effect of Anti-HCV Activity by N-89 or N-251 in Combination with IFN-α and/or RBV

We examined the anti-HCV activity of N-89 or N-251 in combination with IFN-α using OR6 and ORL8 assay systems. The results of the ORL8 assay revealed that the anti-HCV activity of N-89 or N-251 in combination with IFN-α (more than 4 IU/ml) was significantly stronger than that expected as an additive effect, suggesting a synergistic effect of N-89 or N-251 and IFN-α (Fig. 6A). However, such an effect was not clear in the OR6 assay (Fig. S4A). We recently demonstrated that 10 μM (a clinically achievable concentration) of RBV efficiently inhibited HCV-RNA replication in the ORL8 assay [22], and demonstrated that adenosine kinase, which phosphorylates RBV to generate monophosphorylated RBV possessing the inhibitory activity for inosine monophosphate dehydrogenase, is an essential determinant of the anti-HCV activity of RBV in cell culture [23]. Therefore, we next examined the combination effect of RBV in the same way as IFN-α using an ORL8 assay. We observed that the anti-HCV activity of N-89 or N-251 in combination with RBV was significantly stronger than that expected additively, suggesting that there was a synergistic effect between N-89 or N-251 and RBV (Fig. 6B). However, in the OR6 assay, we noticed that RBV showed an additive anti-HCV effect in combination with N-89 or N-251 (Fig. S4B). Since RBV has been shown to have little anti-HCV activity in the OR6 assay system [22], some specific factor(s) in ORL8 cells might contribute to the synergistic effect of N-89 or N-251 in combination with RBV. Therefore, we further examined the effect of N89 or N-251 in combination with both IFN-α and RBV using an ORL8 assay. As expected, the anti-HCV activity of N-89 or N-251 was synergistically enhanced in combination with both IFN-α and RBV in the ORL8 assay (Fig. 6C). On the other hand, in the OR6 assay, a synergistic effect like that seen in the ORL8 assay was not observed (Fig. S4C). We confirmed that any such synergistic effect was not due to the cell toxic effect (Fig. S5).

Discussion

N-89 and its derivative N-251 are preclinical and promising drugs possessing antimalarial activities *in vitro* and *in vivo* comparable to those of artemisinin [26,27]. In the present study, using cell-based HCV-RNA-replication assay systems, we found that N-89 and N-251 possessed potent anti-HCV activities irrespective of the cell lines and HCV strains of genotype 1b, and that they did not work for JFH-1 strain of genotype 2a. Furthermore, We demonstrated that the anti-HCV kinetics of N-89 was faster than that of IFN-α, and that both N-89 and N-251 exhibited synergistic effects in combination with IFN-α and/or RBV.

Along with the worldwide spread of HCV, high prevalence areas of HCV infection have overlapped with endemic areas of malaria infection [39,40]. It is also interesting that the liver is a target organ for the replication of HCV and malaria. This fact would again suggest that N-89 and N-251 target a common factor that is required for the replication of HCV and malaria. At the same time, N-89 and N-251 have become readily and cheaply available due to their ease of synthesis [26,27]. Since we showed that HCV-RNA-replicating cells were cured by monotherapy with N-89, monotherapy with N-89 or N-251 would be simultaneously effective for the diseases caused by malaria and HCV infection. Furthermore, we recently showed that the blood concentration of N-89 or N-251 reaches approximately 1 μM [Kim et al., unpublished data]. Since this concentration, which is equivalent to the EC_{99} value of N-89 in the ORL8 assay, was used for the preparation of cured cells, even monotherapy with N-89 would be useful for patients with chronic hepatitis C.

In regard to the anti-HCV mechanism of N-89 and N-251, we provided evidence that the anti-HCV activity of these reagents was canceled by antioxidant VE, suggesting the induction of oxidative stress. To identify the target factor(s) located downstream of ROS production, we attempted microarray analysis using OR6 and ORL8 cells treated with N-89. However, consequently, we failed to obtain the candidate gene indicating the meaningful expression level, although we identified several genes, which were commonly upregulated or downregulated in the N-89-treated cells (Fig. S6). On the other hand, it has been recently reported that *Plasmodium falciparum* endoplasmic reticulum-resident calcium binding protein is a possible target of N-89 and N-251 [41]. Therefore, this protein may be involved in the anti-HCV activities of N-89 and N-251. To clarify the factor(s), further analysis will be needed.

The synergistic anti-HCV effect of N-89 or N-251 in combination with RBV rather than IFN-α is also interesting. Using RBV-sensitive ORL8 cells, we recently clarified that the anti-HCV mechanism of RBV was mediated by the inhibition of IMPDH, which is required for HCV-RNA replication [22]. In addition, since RBV is an important component of current IFN-based therapies, including the recently developed triple therapy, the use of N-89 or N-251 may further enhance the SVR rate achieved with the current therapy. Furthermore, recent report [42] that the *lead-in* four weeks of RBV treatment before starting a standard course of PEG-IFN with RBV led a weak decrease of viral replication (0.5 ± 0.5 $\log_{10}$) is noteworthy. To evaluate this possibility, we compared the SI values of N-89, N-251, RBV, and CsA using the ORL8 assay system. The results revealed that the SI values of N-89, N-251, RBV, and CsA were 26, 13, 10, and 15, respectively, indicating that the anti-HCV activity of N-89 or N-251 is equivalent to that of RBV or CsA. Since the treatment with N-89/N-251 and RBV exhibits a synergistic effect, oral N-89 or N-251 would be good compounds for inclusion in the current triple therapy.

In conclusion, we found that two oral antimalarial drugs in the preclinical stage of development (N-89 and N-251) exhibited strong anti-HCV activities to genotype 1b. These compounds would have potential as one component of a therapeutic regimen based on combinations of HCV-specific inhibitors.

Supporting Information

Figure S1 Anti-HCV activities of N-89 and N-251 detected in the several assay systems using genome-length HCV-RNA or HCV subgenomic replicon RNA. (A) Effects of N-89 and N-251 on genome-length HCV-RNA (AH1 strain of genotype 1b) replication in the AH1R assay. AH1R cells were treated with N-89 or N-251 for 72 hrs, followed by RL assay (black circles) and WST-1 assay (open triangles). The relative value (%) calculated at each point, when the level in non-treated cells was assigned as 100%, is presented here. Data are expressed as the means ± standard deviation of triplicate assays. (B) Effects of N-89 and N-251 on genome-length HCV-RNA (HCV 1B-4 strain of genotype 1b) replication in the 1B-4R assay. The RL assay and WST-1 assay were performed as described in (A). (C) Effects of N-89 and N-251 on genome-length HCV-RNA (HCV 1B-4 strain of

genotype 1b) replication in the 1B-4RL assay. The RL assay and WST-1 assay were performed as described in (A). (D) Effects of N-89 and N-251 on genome-length HCV-RNA (HCV KAH5 strain of genotype 1b) replication in the KAH5RL assay. The RL assay and WST-1 assay were performed as described in (A). (E) Effects of N-89 and N-251 on HCV subgenomic replicon RNA (HCV O strain of genotype) replication in the sOR assay. The RL assay and WST-1 assay were performed as described in (A). (F) Effects of N-89 and N-251 on HCV subgenomic replicon RNA (HCV O strain of genotype 1b) replication in the sORL8 assay. The RL assay and WST-1 assay were performed as described in (A). (G) Effects of N-89 and N-251 on HCV subgenomic replicon RNA (HCV O strain of genotype 1b) replication in the sORL11 assay. The RL assay and WST-1 assay were performed as described in (A).
(TIF)

Figure S2 No inhibition of RL activity by N-89 or N-251. (A) N-89 and N-251 did not inhibit the RL activity in the OR6 cell lysate. N-89 or N-251 was added to the OR6 cell lysate, and then an RL assay was performed. (B) N-89 and N-251 did not inhibit the RL activity in the ORL8 cell lysate. N-89 or N-251 was added to the ORL8 cell lysate, and then an RL assay was performed.
(TIF)

Figure S3 N-251 did not inhibit the HCV-JFH-1 replication. RSc and D7 cells were inoculated with supernatant from RSc cells replicating JR/C5B/BX-2 [2]. The RL assay was performed as described in Fig. S1A.
(TIF)

Figure S4 Anti-HCV effects of N-89 or N-251 in combination with IFN-α and/or RBV on HCV-RNA replication in OR6 cells. Open symbols in the broken lines show the values expected as an additive anti-HCV effect and closed symbols in the solid lines show the values obtained by the OR6 assay. (A) Effect of N-89 or N-251 in combination with IFN-α on OR6 assay. OR6 cells were treated with N-89 (upper panel) or N-251 (lower panel) in combination with IFN-α for 72 hrs and subjected to RL assay. (B) Effect of N-89 or N-251 in combination with RBV on OR6 assay. OR6 cells were treated with N-89 (upper panel) or N-251 (lower panel) in combination with RBV for 72 hrs and subjected to RL assay. (C) Effect of N-89 or N-251 in combination with IFN-α and RBV on OR6 assay. OR6 cells were treated with N-89 (upper panel) or N-251 (lower panel) in combination with IFN-α and RBV for 72 hrs and subjected to RL assay.
(TIF)

Figure S5 Effects of N-89 or N-251 in combination with IFN-α and/or RBV on the growth of ORL8 or OR6 cells. ORL8 cells (A, B) or OR6 cells (C, D) were treated with N-89 (A, C) or N-251 (B, D) in combination with IFN-α for 72 hrs and subjected to the cell counting. The cell counting was carried out as described in the Supporting Materials and methods.
(TIF)

Figure S6 Selection of genes whose expression levels were commonly upregulated or downregulated in the N-89-treated OR6 and ORL8 cells. (A) Genes whose expression levels were upregulated at ratios of more than 2 in the case of OR6(−) versus OR6(N-89) or ORL8(−) versus ORL8(N-89) were selected. 4 genes upregulated commonly in the N-89-treated cells were listed. (B) Genes whose expression levels were downregulated at ratios of less than 0.5 in the case of OR6(−) versus OR6(N-89) or ORL8(−) versus ORL8(N-89) were selected. 5 genes downregulated commonly in the N-89-treated cells were listed.
(TIF)

Text S1.
(DOC)

Acknowledgments

We thank Yoshimi Kawae for her technical assistances. We also thank Dr. Hiroyuki Doi (Okayama University, Japan) for his helpful suggestions.

Author Contributions

Conceived and designed the experiments: YU NK. Performed the experiments: YU MT. Analyzed the data: YU NK. Contributed reagents/materials/analysis tools: KM HD TW HSK AS YW MI. Wrote the paper: YU NK.

References

1. Thomas DL (2000) Hepatitis C epidemiology. Curr Top Microbiol Immunol 242: 25–41.
2. Kato N (2001) Molecular virology of hepatitis C virus. Acta Med Okayama 55: 133–159.
3. Kato N, Hijikata M, Ootsuyama Y, Nakagawa M, Ohkoshi S, et al. (1990) Molecular cloning of the human hepatitis C virus genome from Japanese patients with non-A, non-B hepatitis. Proc Natl Acad Sci U S A 87: 9524–9528.
4. Chevaliez S, Pawlotsky JM (2007) Interferon-based therapy of hepatitis C. Adv Drug Deliv Rev 59: 1222–1241.
5. Ghany MG, Nelson DR, Strader DB, Thomas DL, Seeff LB (2011) An update on treatment of genotype 1 chronic hepatitis C virus infection: 2011 practice guideline by the American Association for the Study of Liver Diseases. Hepatology 54: 1433–1444.
6. Jacobson IM, McHutchison JG, Dusheiko G, Di Bisceglie AM, Reddy KR, et al. (2011) Telaprevir for previously untreated chronic hepatitis C virus infection. N Engl J Med 364: 2405–2416.
7. Poordad F, McCone J Jr, Bacon BR, Bruno S, Manns MP, et al. (2011) Boceprevir for untreated chronic HCV genotype 1 infection. N Engl J Med 364: 1195–1206.
8. Reesink HW, Zeuzem S, Weegink CJ, Forestier N, van Vliet A, et al. (2006) Rapid decline of viral RNA in hepatitis C patients treated with VX-950: a phase Ib, placebo-controlled, randomized study. Gastroenterology 131: 997–1002.
9. Susser S, Welsch C, Wang Y, Zettler M, Domingues FS, et al. (2009) Characterization of resistance to the protease inhibitor boceprevir in hepatitis C virus-infected patients. Hepatology 50: 1709–1718.
10. Rosen HR (2011) Clinical practice. Chronic hepatitis C infection. N Engl J Med 364: 2429–2438.
11. Pawlotsky JM (2011) Treatment failure and resistance with direct-acting antiviral drugs against hepatitis C virus. Hepatology 53: 1742–1751.
12. Bartenschlager R, Sparacio S (2007) Hepatitis C virus molecular clones and their replication capacity in vivo and in cell culture. Virus Res 127: 195–207.
13. Ikeda M, Abe K, Dansako H, Nakamura T, Naka K, et al. (2005) Efficient replication of a full-length hepatitis C virus genome, strain O, in cell culture, and development of a luciferase reporter system. Biochem Biophys Res Commun 329: 1350–1359.
14. Ikeda M, Kato N (2007) Modulation of host metabolism as a target of new antivirals. Adv Drug Deliv Rev 59: 1277–1289.
15. Moradpour D, Penin F, Rice CM (2007) Replication of hepatitis C virus. Nat Rev Microbiol 5: 453–463.
16. Naka K, Ikeda M, Abe K, Dansako H, Kato N (2005) Mizoribine inhibits hepatitis C virus RNA replication: effect of combination with interferon-alpha. Biochem Biophys Res Commun 330: 871–879.
17. Ikeda M, Abe K, Yamada M, Dansako H, Naka K, et al. (2006) Different anti-HCV profiles of statins and their potential for combination therapy with interferon. Hepatology 44: 117–125.
18. Nozaki A, Morimoto M, Kondo M, Oshima T, Numata K, et al. (2010) Hydroxyurea as an inhibitor of hepatitis C virus RNA replication. Arch Virol 155: 601–605.
19. Ikeda M, Kawai Y, Mori K, Yano M, Abe K, et al. (2011) Anti-ulcer agent teprenone inhibits hepatitis C virus replication: potential treatment for hepatitis C. Liver Int 31: 871–880.
20. Kato N, Mori K, Abe K, Dansako H, Kuroki M, et al. (2009) Efficient replication systems for hepatitis C virus using a new human hepatoma cell line. Virus Res 146: 41–50.
21. Mori K, Ikeda M, Ariumi Y, Kato N (2010) Gene expression profile of Li23, a new human hepatoma cell line that enables robust hepatitis C virus replication: Comparison with HuH-7 and other hepatic cell lines. Hepatol Res 40: 1248–1253.

22. Mori K, Ikeda M, Ariumi Y, Dansako H, Wakita T, et al. (2011) Mechanism of action of ribavirin in a novel hepatitis C virus replication cell system. Virus Res 157: 61–70.
23. Mori K, Hiraoka O, Ikeda M, Ariumi Y, Hiramoto A, et al. (2013) Adenosine kinase is a key determinant for the anti-HCV activity of ribavirin. Hepatology in press.
24. Ueda Y, Mori K, Ariumi Y, Ikeda M, Kato N (2011) Plural assay systems derived from different cell lines and hepatitis C virus strains are required for the objective evaluation of anti-hepatitis C virus reagents. Biochem Biophys Res Commun 409: 663–668.
25. Paeshuyse J, Coelmont L, Vliegen I, Van Hemel J, Vandenkerckhove J, et al. (2006) Hemin potentiates the anti-hepatitis C virus activity of the antimalarial drug artemisinin. Biochem Biophys Res Commun 348: 139–144.
26. Kim HS, Nagai Y, Ono K, Begum K, Wataya Y, et al. (2001) Synthesis and antimalarial activity of novel medium-sized 1,2,4,5-tetraoxacycloalkanes. J Med Chem 44: 2357–2361.
27. Sato A, Hiramoto A, Morita M, Matsumoto M, Komich Y, et al. (2011) Antimalarial activity of endoperoxide compound 6-(1,2,6,7-tetraoxaspiro[7.11]-nonadec-4-yl)hexan-1-ol. Parasitol Int 60: 270–273.
28. Sato A, Kawai S, Hiramoto A, Morita M, Tanigawa N, et al. (2011) Antimalarial activity of 6-(1,2,6,7-tetraoxaspiro[7.11]nonadec-4-yl)hexan-1-ol (N-251) and its carboxylic acid derivatives. Parasitol Int 60: 488–492.
29. Takeda M, Ikeda M, Ariumi Y, Wakita T, Kato N (2012) Development of hepatitis C virus production reporter-assay systems using two different hepatoma cell lines. J Gen Virol 93: 1422–1431.
30. Mori K, Ueda Y, Ariumi Y, Dansako H, Ikeda M, et al. (2012) Development of a drug assay system with hepatitis C virus genome derived from a patient with acute hepatitis C. Virus Genes 44: 374–381.
31. Nishimura G, Ikeda M, Mori K, Nakazawa T, Ariumi Y, et al. (2009) Replicons from genotype 1b HCV-positive sera exhibit diverse sensitivities to anti-HCV reagents. Antiviral Res 82: 42–50.
32. Kato N, Sugiyama K, Namba K, Dansako H, Nakamura T, et al. (2003) Establishment of a hepatitis C virus subgenomic replicon derived from human hepatocytes infected in vitro. Biochem Biophys Res Commun 306: 756–766.
33. Aly NS, Hiramoto A, Sanai H, Hiraoka O, Hiramoto K, et al. (2007) Proteome analysis of new antimalarial endoperoxide against Plasmodium falciparum. Parasitol Res 100: 1119–1124.
34. Kim HS, Begum K, Ogura N, Wataya Y, Nonami Y, et al. (2003) Antimalarial activity of novel 1,2,5,6-tetraoxacycloalkanes and 1,2,5-trioxacycloalkanes. J Med Chem 46: 1957–1961.
35. Mori K, Abe K, Dansako H, Ariumi Y, Ikeda M, et al. (2008) New efficient replication system with hepatitis C virus genome derived from a patient with acute hepatitis C. Biochem Biophys Res Commun 371: 104–109.
36. Abe K, Ikeda M, Dansako H, Naka K, Kato N (2007) Cell culture-adaptive NS3 mutations required for the robust replication of genome-length hepatitis C virus RNA. Virus Res 125: 88–97.
37. Yano M, Ikeda M, Abe K, Dansako H, Ohkoshi S, et al. (2007) Comprehensive analysis of the effects of ordinary nutrients on hepatitis C virus RNA replication in cell culture. Antimicrob Agents Chemother 51: 2016–2027.
38. Yano M, Ikeda M, Abe K, Kawai Y, Kuroki M, et al. (2009) Oxidative stress induces anti-hepatitis C virus status via the activation of extracellular signal-regulated kinase. Hepatology 50: 678–688.
39. Feachem RG, Phillips AA, Hwang J, Cotter C, Wielgosz B, et al. (2010) Shrinking the malaria map: progress and prospects. Lancet 376: 1566–1578.
40. Shepard CW, Finelli L, Alter MJ (2005) Global epidemiology of hepatitis C virus infection. Lancet Infect Dis 5: 558–567.
41. Morita M, Sanai H, Hiramoto A, Sato A, Hiraoka O, et al. (2012) Plasmodium falciparum endoplasmic reticulum-resident calcium binding protein is a possible target of synthetic antimalarial endoperoxides, N-89 and N-251. J Proteome Res 11: 5704–5711.
42. Rotman Y, Noureddin M, Feld JJ, Guedj J, Witthaus M, et al. (2013) Effect of ribavirin on viral kinetics and liver gene expression in chronic hepatitis C. Gut in press.

Cell Transplantation, Vol. 22, pp. 1695–1708, 2013

0963-6897/13 $90.00 + .00
DOI: http://dx.doi.org/10.3727/096368912X657738
E-ISSN 1555-3892
www.cognizantcommunication.com

Adoptive Transfer of Allogeneic Liver Sinusoidal Endothelial Cells Specifically Inhibits T-Cell Responses to Cognate Stimuli

Masataka Banshodani, Takashi Onoe, Masayuki Shishida, Hiroyuki Tahara, Shinji Hashimoto, Yuka Igarashi, Yuka Tanaka, and Hideki Ohdan

Department of Surgery, Division of Frontier Medical Science, Programs for Biomedical Research, Graduate School of Biomedical Sciences, Hiroshima University, Minami-ku, Hiroshima, Japan

Although it is well known that liver allografts are often accepted by recipients, leading to donor-specific tolerance of further organ transplants, the underlying mechanisms remain unclear. We had previously used an in vitro model and showed that mouse liver sinusoidal endothelial cells (LSECs) selectively suppress allospecific T-cells across major histocompatibility complex (MHC) barriers. In the present study, we established an in vivo model for evaluating the immunomodulatory effects of allogeneic LSECs on corresponding T-cells. Allogeneic BALB/cA LSECs were injected intraportally into recombination activating gene 2 γ-chain double-knockout (RAG2/gc-KO, H-2^b) mice lacking T, B, and natural killer (NK) cells. In order to facilitate LSEC engraftment, the RAG2/gc-KO mice were injected intraperitoneally with monocrotaline 2 days before the adoptive transfer of LSECs; this impaired the host LSECs, conferring a proliferative advantage to the transplanted LSECs. After orthotopic allogeneic LSEC engraftment, the RAG2/gc-KO mice were immune reconstituted intravenously with C57BL/6 splenocytes. After immune reconstitution, mixed lymphocyte reaction (MLR) assay using splenocytes from the recipients revealed that specific inhibition of host CD4$^+$ and CD8$^+$ T-cell proliferation was greater in response to allostimulation with irradiated BALB/cA splenocytes rather than to stimulation with irradiated third party SJL/jorllco splenocytes. This inhibitory effect was attenuated by administering anti-programmed death ligand 1 (PD-L1) monoclonal antibody during immune reconstitution in the above-mentioned mice, but not in RAG2/gc-KO mice engrafted with Fas ligand (FasL)-deficient BALB/cA LSECs. Furthermore, engraftment of allogeneic BALB/cA LSECs significantly prolonged the survival of subsequently grafted cognate allogeneic BALB/cA hearts in RAG2/gc-KO mice immune reconstituted with bone marrow transplantation from C57BL/6 mice. In conclusion, murine LSECs have been proven capable of suppressing T-cells with cognate specificity for LSECs in an in vivo model. The programmed death 1/PD-L1 pathway is likely involved in these suppressive effects.

Key words: Endothelial cells; Tolerance; Transplantation; Alloreactive T-cells; Programmed death ligand 1 (PD-L1)

INTRODUCTION

Liver allografts are well accepted across major histocompatibility complex (MHC) barriers without immunosuppression in some species (5,6,10). The presence of a liver allograft can suppress the rejection of other solid tissue grafts (e.g., heart and skin) from the same donor (1); hence, the liver appears to favor immune tolerance rather than immunity. The mechanisms underlying such immune tolerance may be mediated by innate and adaptive immune regulators (26). We recently demonstrated a novel relevant mechanism of this liver allograft tolerance: naive allogeneic liver sinusoidal endothelial cells (LSECs) selectively inhibit cluster of differentiation 4 positive (CD4$^+$) and CD8$^+$ T-cells with direct allospecificity in mice in which liver allografts are normally accepted without recipient immune suppression across MHC barriers (22,23). Naive LSECs in mice constitutively express all molecules necessary for antigen presentation; that is, freshly isolated LSECs express MHC class II, CD40, CD80, and CD86 but do not induce allogeneic T-cell proliferation (22). In an allogeneic mixed hepatic constituent cell-lymphocyte reaction assay. Marked proliferation of reactive CD4$^+$ and CD8$^+$ T-cells was observed when LSECs were depleted from the hepatic constituent cell stimulators (23). The sinusoidal architecture, in which circulating leukocytes are forced into frequent contact with LSECs due to the small sinusoid diameter (7–12 μm), most likely promotes the immunomodulatory activity of

Received June 28, 2011; final acceptance August 25, 2012. Online prepub date: October 8, 2012.
Address correspondence to Hideki Ohdan, M.D., Ph.D., Department of Surgery, Division of Frontier Medical Science, Programs for Biomedical Research, Graduate School of Biomedical Sciences, Hiroshima University, 1-2-3 Kasumi, Minami-ku, Hiroshima 734-8551, Japan. Tel: +81-82-257-5220; Fax: +81-82-257-5224; E-mail: hohdan@hiroshima-u.ac.jp

LSECs against alloreactive T-cells. Such an interpretation, which is based on in vitro results, raised the question of whether recipients of isolated allogeneic LSECs, which may have a pivotal tolerogenic property, allospecifically suppress T-cells.

It was recently reported that inoculation with LSECs leads to host liver sinusoidal endothelium repopulation; that is, syngeneic LSECs transplanted into the liver via portal vein injection survived only in the liver without redistribution to other organs, including the lungs, heart, spleen, kidney, and intestines (2). By using a similar in vivo model system in the present study, we investigated the suppressive effects of exogenously inoculated allogeneic LSECs on allospecific immune responses. To exclude the possibility that the inoculated LSECs were eliminated by either innate or acquired immunity before achieving engraftment in the liver sinusoidal endothelium, we employed recombination activating gene 2 γ-chain double-knockout (RAG2/gc-KO) mice, which lack natural killer (NK), natural killer T (NKT), T-, and B-cells, as allogeneic LSEC recipients. The allogeneic LSEC chimeric mice were then reconstituted with host-type splenocytes (SPLs) or bone marrow cells (BMCs) to investigate the immune responses of allospecific T-cells.

MATERIALS AND METHODS

Mice

Eight- to 12-week-old female C57BL/6 (B6, H-2^b), BALB/cA (BALB/c, H-2^d), and SJL/jorllco (SJL/j, H-2^s) mice were purchased from Clea Japan (Tokyo, Japan). Female Cpt.C3-Tnfsf6^{gld} mice (BALB/c-gld, H-2^d, BALB/cA background) that were homozygous for the Fas ligand (FasL)^{gld} mutation were purchased from The Jackson Laboratory (Bar Harbor, ME, USA). Age-matched (8- to 12-week-old) mice were used for the experiments. RAG2/gc-KO (H-2^b) mice were purchased from Taconic Farms (Hudson, NY, USA). All animals were maintained under pathogen-free conditions and in compliance with national and institutional guidelines. Animal experiments were approved by the Institutional Review Board of Hiroshima University and were conducted in accordance with the National Institutes of Health guidelines.

LSEC Isolation

Since we previously demonstrated that LSECs exclusively express CD105 at higher levels than the endothelium of the central veins or other vessels in the liver (23,27), CD105$^+$ cells were positively selected for the isolation of LSECs from nonparenchymal cell fractions of the liver. Briefly, the livers of BALB/c or BALB/c-gld mice were perfused with portal injection using the two-step collagenase perfusion method (23,25,28). Disaggregated liver cells were centrifuged at $50 \times g$ for 1 min for hepatocyte removal. The supernatant was subsequently centrifuged at $150 \times g$ for 5 min, and hepatic nonparenchymal cells (HNPCs) were obtained and stained with biotin-conjugated anti-CD105 (MJ7/18, eBioscience, San Diego, CA, USA). The cells were then counterstained with streptavidin microbeads (Miltenyi Biotec, Bergisch Gladbach, Germany) and magnetically sorted using an automated magnetic cell sorter (autoMACS, Miltenyi Biotec). This sorting technique yielded $4.8 \pm 0.5 \times 10^6$ cells/body in the positive fraction, with $97.9 \pm 0.3\%$ purity ($n=4$), indicating that marginal contamination with cells other than LSECs could not be ruled out.

Surface Marker Analyses of Freshly Isolated LSECs

The CD105$^+$ LSECs were freshly isolated from BALB/c mice. The expression levels of H-2K^d/H-2D^d (MHC-class I), I-A/I-E (MHC-class II), CD80, CD146, FasL, and CD274 [programmed death ligand 1 (PD-L1)] were measured by flow cytometry (FCM; see later).

Orthotopic LSEC Engraftment

Isolated LSECs were prepared as a single-cell suspension. The LSECs (4×10^6 cells) in 0.5 ml of Medium 199 (Sigma-Aldrich, Saint Louis, MO, USA) containing 1% *N*-2-hydroxyethylpiperazine-*N'*-2-ethanesulfonic acid (HEPES) buffer (GIBCO; Invitrogen, Carlsbad, CA, USA) were injected into each recipient RAG2/gc-KO mouse through the portal vein using a 30-gauge needle. Medium 199 containing 1% HEPES buffer without LSECs was injected into control recipient RAG2/gc-KO mice. In some experiments, we administered monocrotaline (MCT; Sigma-Aldrich), a genotoxic pyrrolizidine alkaloid that impairs the host LSECs and confers a proliferative advantage on the transplanted LSECs. It was previously discovered that MCT injection to recipients prior to LSEC inoculation markedly accelerated the engraftment of inoculated LSECs, but that MCT-induced endothelial injury in additional vascular beds did not promote inoculated LSEC survival in extrahepatic locations (7). Two days before the adaptive transfer of LSECs, a 200–300 mg/kg dose of MCT was intraperitoneally injected into recipient RAG2/gc-KO mice to facilitate transplanted LSEC engraftment. The RAG2/gc-KO mice that received the same dose of MCT alone were used as controls. To evaluate orthotopic engraftment of transplanted allogeneic BALB/c LSECs in the recipient liver, the livers were immunostained using fluorescein isothiocyanate (FITC)-conjugated H-2K^d/H-2D^d monoclonal antibody (mAb) (34-1-2S; Beckman Coulter, Fullerton, CA, USA), phycoerythrin (PE)-conjugated anti-mouse CD146 (Abcam, Cambridge, UK), and anti-CD274-PE (MIH5; BD Pharmingen, San Diego, CA, USA) mAbs and examined with a fluorescence microscope (BZ-8000; KEYENCE, Osaka, Japan). To quantify LSEC

chimerism, HNPCs were reisolated from the livers of the recipients of BALB/c LSECs. For the FCM analyses, the LSECs were selected by gating on CD105$^+$ cells, and the proportion of cells expressing H-2K^d/H-2D^d (MHC-class I) among all of the LSECs was determined.

Immune Reconstitution of Recipient RAG2/gc-KO Mice

Immune reconstitution of the immunodeficient mice was performed by use of the method described previously (32). In brief, B6 SPLs (2×10^7) in 0.5 ml of Medium 199 containing 1% HEPES buffer were injected into recipient RAG2/gc-KO mice through the tail vein for immune reconstitution after engraftment of LSECs from either BALB/c or BALB/c-gld mice. In some in vivo experiments, to block PD-L1, recipient mice were pretreated with 500 μg of anti-PD-L1 blocking mAb (MIH5; eBioscience) or rat IgG isotype control antibody (Ab) (Beckman Coulter) just before immune reconstitution, and these antibodies were readministered 3 days later. One week after SPL inoculation, the recipient mice were sacrificed, and SPLs were obtained for subsequent mixed lymphocyte reaction (MLR) assay. In some experiments, bone marrow transplantation (BMT) was performed from B6 mice to recipient RAG2/gc-KO mice after LSEC engraftment. Briefly, recipient RAG2/gc-KO mice were irradiated (3 Gy) and injected with BMCs (1×10^7 cells/mouse) from B6 mice through the tail vein. After SPL inoculation or BMT, peripheral blood mononuclear cells (PBMCs) were obtained from recipient mice, and the CD4$^+$ T, CD8$^+$ T, NK, and NKT cell immune reconstitution levels were evaluated by FCM. Immune reconstituted recipient RAG2/gc-KO mice were used at least 6 weeks after BMT for the subsequent heart transplant experiment. Mice that did not receive LSECs but were immune reconstituted with either SPLs or BMCs were used as controls for subsequent studies.

CFSE-MLR Assay

SPLs obtained from B6 (syngeneic stimulator), BALB/c (allogeneic stimulator), or SJL/j (third-party stimulator) mice were irradiated with 30 Gy and used as stimulator cells. For MLR using the carboxyfluorescein diacetate succinimidyl ester (CFSE) labeling technique (CFSE-MLR), SPLs from immune reconstituted recipient RAG2/gc-KO mice were labeled with 5 μM CFSE (Molecular Probes, Eugene, OR, USA) as described previously (21) and resuspended in culture medium as responder cells. The stimulator (2×10^6 cells) and responder (2×10^6 cells) cells were cocultured (1:1 ratio) in a total volume of 1 ml of medium in 48-well flat-bottom plates at 37°C in an incubator with an atmosphere of 5% CO_2 in the dark for 4.5 days. In the resulting CFSE fluorescence histograms, CD4$^+$ and CD8$^+$ T-cells were selected by gating and analyzed for CFSE fluorescence. The numbers of division precursors and mitotic events of alloreactive T-cells were mathematically determined using logarithmic CFSE intensity on the basis of the peak of the undivided cells, while the mitotic index was calculated by dividing the total number of mitotic events by the total number of precursors (21). The T-cell stimulation index was calculated by dividing the mitotic index of T-cells responding to allogeneic or third-party SPLs by that of T-cells responding to the syngeneic SPLs.

FCM Analyses

The following reagents were used for surface staining: anti-CD3-FITC (145-2c11), anti-CD4-FITC (GK1.5), anti-CD8-FITC (53-6.7), anti-CD80-FITC (16-10A1), anti-I-A/I-E-FITC (2G9), anti-CD4-PE (GK1.5), anti-CD8-PE (53-6.7), anti-CD274-PE (MIH5), anti-mouse H-2K^d/H-2D^d-PE (SF1-1.1), anti-CD4-biotin (RM4-5), anti-CD8-biotin (53-6.7), anti-CD44-biotin (IM7), anti-CD45RB-biotin (16A), anti-CD62L-biotin (MEL-14), anti-CD105-biotin (MJ7/18), anti-NK1.1-allophycocyanin (PK136) mAbs, isotype-matched control Abs, streptavidin-allophycocyanin (BD Pharmingen), anti-CD146-FITC (ME-9F1; Miltenyi Biotec), FITC-conjugated mouse (C3H/HeJ) anti-mouse H-2K^d/H-2D^d (34-1-2S; Beckman Coulter), and anti-FasL-PE mAbs (MFL3; eBioscience). All analyses were performed using a FACSCalibur (BD Biosciences, San Jose, CA, USA). Nonspecific Fc-γ receptor binding of labeled mAbs was blocked by purified rat anti-mouse CD16/CD32 mAb (mouse BD Fc block) (2.4G2; BD Pharmingen). Dead cells were excluded from the analysis by forward scatter and propidium iodide (Sigma-Aldrich).

Heterotopic Heart Transplantation

Cervical heterotopic heart transplantation from BALB/c or SJL/j mice into the immune reconstituted recipient RAG2/gc-KO mice was performed using a modified cuff technique (20). Briefly, the right external jugular vein and the right common carotid artery were dissected free and fixed to the appropriate cuffs composed of polyethylene tubes (2.5F, Portex Ltd., London, UK). For anastomoses, the aorta and the main pulmonary artery of the obtained donor heart were drawn over the end of the common carotid artery and the external jugular vein, respectively. The graft ischemic time for the transplanted hearts was <30 min. Graft function was monitored by daily inspection and palpation. Rejection, defined as cessation of graft beating, was confirmed by histological analysis.

Statistical Analyses

The results were analyzed statistically by using Student's t test or the log-rank test for graft survival. Data are expressed as mean ± standard error of the mean (SEM). A value of $p<0.05$ was considered statistically significant.

RESULTS

Allogeneic LSEC Engraftment Was Successfully Achieved In Vivo

Previous studies have shown that allogeneic LSECs render allospecific T-cells hyporesponsive in vitro (22,23). In order to test the immunoregulatory effects of LSECs in vivo, we generated an LSEC engraftment model in which RAG2/gc-KO mice were orthotopically engrafted with allogeneic BALB/c LSECs (4×10^6 cells/mouse) and then immunologically reconstructed using SPLs (2×10^7 cells/mouse) from B6 mice 1 week after the LSEC inoculation. The inoculated LSECs were barely detected in the host liver sinusoid 2 weeks after inoculation in immunohistochemical studies using anti-H-2K^d/H-2D^d Ab (Fig. 1B). LSEC engraftment was successfully increased by MCT administration 2 days prior to the inoculation. A significant proportion of LSECs was stably detected even 7 weeks after LSEC inoculation in MCT-pretreated mice (Fig. 1C). By merging these immunofluorescence microscopic findings, we confirmed that the engrafted cells that were stained with anti-H-2K^d/H-2D^d Ab presented on the lining of the hepatic sinusoid face to the sinusoidal lumen and also were stained with anti-CD146 mAb, which is a LSEC-specific marker (Fig. 1D, E). The FCM analyses consistently revealed that MCT pretreatment enhanced LSEC engraftment; that is, the LSEC chimerism level increased (Fig. 2A, B). Immune reconstitution was confirmed by the presence of both CD4$^+$ and CD8$^+$ T-cells in the spleens of recipient RAG2/gc-KO mice by FCM 1 week after SPL inoculation. There was no statistically significant difference in the degree of CD4$^+$ and CD8$^+$ T-cell reconstitution between recipient mice with allogeneic LSECs and corresponding control mice without allogeneic LSECs (Fig. 3).

Orthotopic Engraftment of Allogeneic LSEC Led to Specific Inhibition of T-Cells Responding to Stimulation Cognate With LSECs

In order to address whether orthotopic engraftment of MHC-disparate allogeneic LSECs in the MCT-pretreated mice can induce specific inhibition of alloreactive T-cells after immune reconstitution with MHC-matched SPLs,

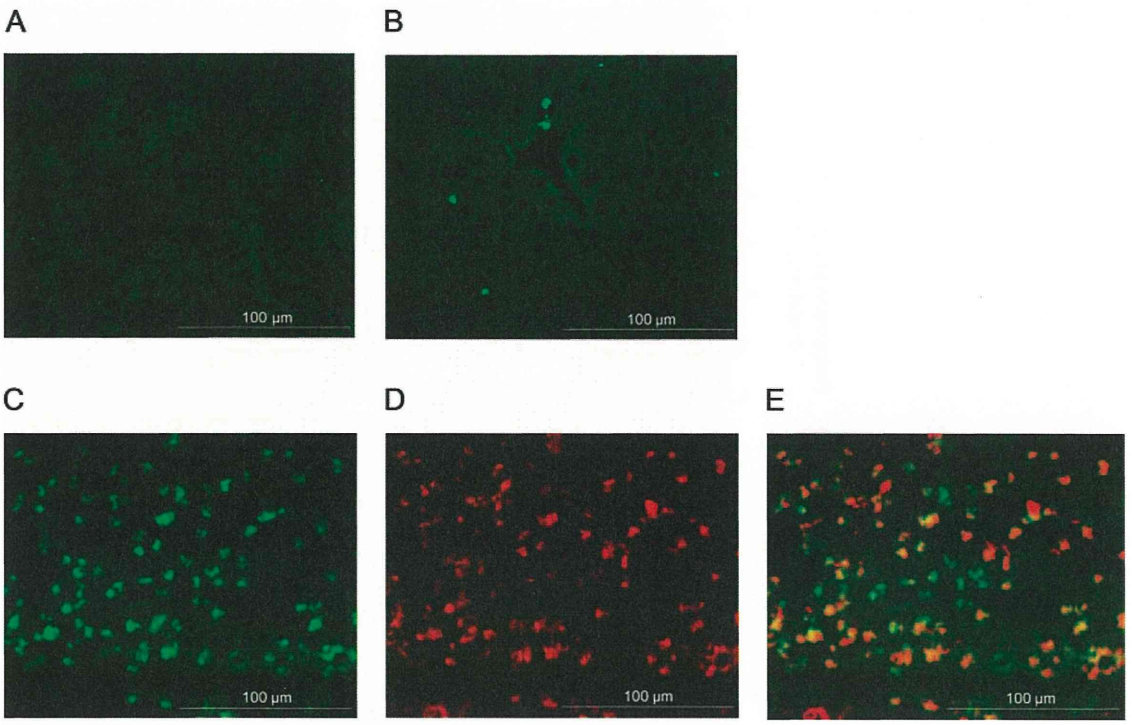

Figure 1. An in vivo liver sinusoidal endothelial cell (LSEC) engraftment model was established using allogeneic BALB/c LSECs that were transferred to RAG2/gc-KO mice through the portal vein. Recipient recombination activating gene 2 γ-chain double-knockout (RAG2/gc-KO) mouse livers were immunostained with fluorescein isothiocyanate (FITC)-conjugated anti-mouse major histocompatibility complex class I (H-2K^d/H-2D^d) (A–C) and phycoerythrin (PE)-conjugated anti-mouse cluster of differentiation 146 (CD146) monoclonal antibodies (mAbs) (D) for identification of transferred LSECs in the liver. (A) Livers from control RAG2/gc-KO mice that did not receive allogeneic BALB/c LSECs. (B) A few transferred LSECs were identified in the liver sinusoids 2 weeks after LSEC inoculation in recipient mice without monocrotaline (MCT). (C) Increased engraftment of the transferred LSECs was identified 7 weeks after LSEC inoculation in recipient mice pretreated with MCT. (D) Endothelial cells were immunostained with CD146 mAb. (E) Merged image of (C) and (D). The figures shown are representative of three independent experiments.

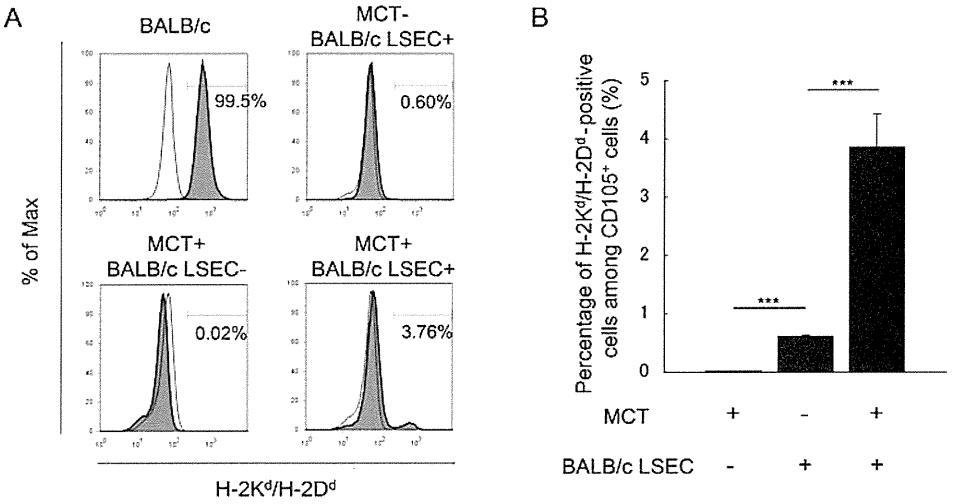

Figure 2. MCT pretreatment enhanced allogeneic LSEC engraftment. The RAG2/gc-KO mice were injected with BALB/c LSECs 2 days after the MCT pretreatment. Six weeks after the LSEC inoculation, hepatic nonparenchymal cells were reisolated from the recipient mice and stained for CD105 and H-2K^d/H-2D^d to analyze the donor-type MHC class I expression in the CD105$^+$ LSECs by flow cytometry (FCM). (A) A representative figure in each group is shown. The thin and filled lines represent staining with isotype-matched control antibody (Ab) and anti-H-2K^d/H-2D^d mAb, respectively. The percent of Max is the number of cells in each bin of the histograms divided by the number of cells in the bin that contains the largest number of cells. The FCM profile from one experimental animal among four or five animals in each group is shown. (B) The percentages of H-2K^d/H-2D^d-positive cells among all of the CD105$^+$ cells in the liver of the RAG2/gc-KO mouse recipients of BALB/c LSECs were determined by FCM analysis (MCT+, LSEC−: $n=4$; MCT−, LSEC+: $n=5$; MCT+, LSEC+: $n=5$). The mean ± SEM values for the individual groups are shown. ***$p<0.001$.

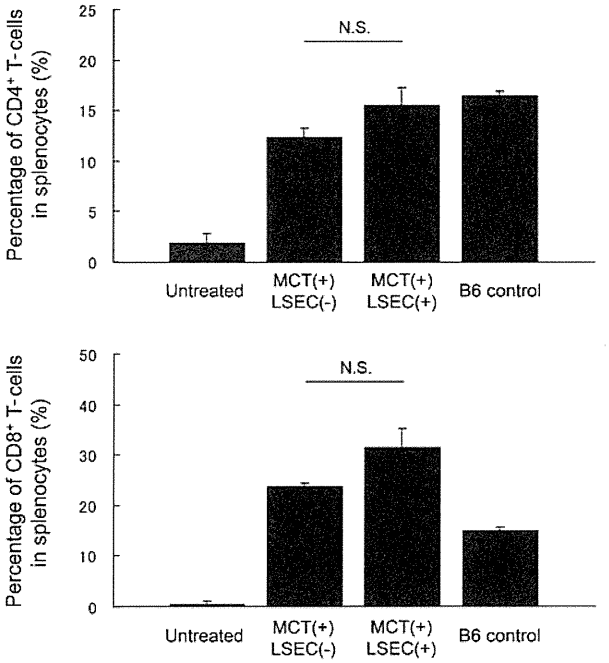

Figure 3. RAG2/gc-KO mice were immune reconstituted using B6 splenocytes (SPLs). BALB/c LSECs were inoculated in MCT-pretreated RAG2/gc-KO mice, and B6 SPLs were injected 6 weeks later. One week after SPL inoculation, the recipient mice were sacrificed, and SPLs were isolated for FCM analysis. Anti-CD4 and anti-CD8 mAbs were used for surface staining of these SPLs. In the FCM analyses, the percentages of CD4$^+$ or CD8$^+$ T-cells in the SPLs were measured in untreated control RAG2/gc-KO mice ($n=3$) (left), immune reconstituted RAG2/gc-KO mice (MCT+, LSEC−: $n=4$; MCT+, LSEC+: $n=4$) (middle), and wild-type (WT) B6 control mice ($n=4$) (right). The frequency of each gated population among total obtained cells is shown.

we analyzed the responsiveness of reconstituted T-cells in MLR assays using the CFSE labeling technique. In syngeneic combinations using B6 SPLs as stimulators, the MLR assay revealed minimal T-cell proliferation in immune reconstituted recipient RAG2/gc-KO mice with and without allogeneic BALB/c LSEC engraftment (Fig. 4A, B). In fully allogeneic combinations using BALB/c SPLs, alloreactive T-cells of immune reconstituted recipient RAG2/gc-KO mice without allogeneic BALB/c LSEC engraftment proliferated markedly, as expected. In the recipient mice with allogeneic BALB/c LSEC engraftment, the response of the anti-BALB/c $CD4^+$ and $CD8^+$ T-cells was significantly less than that of the anti-third-party SJL/j $CD4^+$ and $CD8^+$ T-cells, whereas both responses were similar in the immune reconstituted RAG2/gc-KO control mice without allogeneic LSEC engraftment (Fig. 4C).

The PD-1/PD-L1 Pathway Was Involved in the Suppressive Effects of Engrafted Allogeneic LSECs on Alloreactive $CD4^+$ T-Cells

The phenotypic analysis by FCM revealed that the freshly isolated BALB/c LSECs constitutively expressed FasL and PD-L1, which are death ligands, as well as MHC classes I and II and CD80, which are necessary for antigen-presenting cells (APCs), and CD146 (LSEC-specific marker) at the time of LSEC inoculation (Fig. 5). Hence, we explored the possibility that the Fas/FasL or programmed death 1 (PD-1)/PD-L1 pathway plays a role in the suppressive effect of LSECs on alloreactive T-cells in an in vivo model. FasL-deficient BALB/c (BALB/c-gld) LSECs were inoculated into RAG2/gc-KO mice after MCT treatment, and these mice were then immune reconstituted using B6 SPLs. The MLR assay utilizing SPLs from those mice revealed marked inhibition of alloreactive T-cell proliferation; that is, the stimulation indices of the anti-BALB/c $CD4^+$ and $CD8^+$ T-cells were still significantly less than those of third-party-reactive $CD4^+$ and $CD8^+$ T-cells in mice with BALB/c-gld LSECs (Fig. 6). In a separate experiment, LSECs from BALB/c mice were inoculated into RAG2/gc-KO mice, and then anti-PD-L1-blocking mAb was injected at 3-day intervals during immune reconstitution. Administration of anti-PD-L1-blocking mAb abrogated specific inhibition of the anti-BALB/c $CD4^+$ T-cell response. Since PD-L1 expressed on host native LSECs also likely plays a significant role in the inhibition of self-reactive T-cells, the administration of anti-PD-L1 blocking mAb may interfere with control T-cell responses to syngeneic stimuli. In fact, the control anti-B6 T-cell responses in the anti-PD-L1 mAb-treated group were somewhat higher than those in the isotype-matched control Ab-treated group (data not shown). This result explains why anti-BALB/c responses were seemingly unaltered and anti-SJL T-cell responses were seemingly suppressed in the anti-PD-L1 mAb-treated group, compared to those in the isotype control Ab-treated group. Unexpectedly, administration of the isotype-matched control Ab did not result in any anti-BALB/c $CD8^+$ T-cell inhibition, which suggested that the injected IgG interfered with these effects on $CD8^+$ T-cells (Fig. 7A). $CD8^+$ T-cells express Fc receptors for IgG (FcγR), but $CD4^+$ T-cells do not, in response to certain stimuli (9); therefore, the Fc part of the injected IgG possibly binds FcγR on $CD8^+$ T-cells, leading to interference with the LSEC-induced inhibitory effects on $CD8^+$ T-cells. Thus, at least in alloreactive $CD4^+$ T-cells, the PD-1/PD-L1 pathway could be involved in the suppressive effects of orthotopically engrafted allogeneic LSECs. Supporting this idea, immunohistochemical staining revealed that the engrafted allogeneic LSECs persistently expressed PD-L1 even 7 weeks after the inoculation (Fig. 7B).

Engraftment of Allogeneic LSECs Prolonged Survival of Subsequently Grafted Cognate Allogeneic Hearts in RAG2/gc-KO Mice Immune Reconstituted by BMT

It has been shown that the presence of a liver allograft can suppress rejection of other organ grafts from the same donor (1). To address the possibility that allogeneic LSECs play a role in such immunoregulatory effects on subsequently transplanted organs, allogeneic hearts from BALB/c mice were transplanted into immune reconstituted recipient RAG2/gc-KO mice in which allogeneic LSECs from BALB/c mice had been engrafted after MCT pretreatment. When heart allografts from BALB/c mice were transplanted to the recipients 1 week after B6 SPL inoculation for immune reconstitution, LSEC engraftment did not result in prolonged heart allograft survival (data not shown).

One possible explanation for the failure to prevent allograft heart rejection in mice immune reconstituted with SPLs is that extensive T-cell proliferation occurred after the adoptive transfer of mature T-cells in immune-deficient mice; this process, termed homeostatic proliferation, might lead to insusceptibility of those T-cells to LSEC-induced suppression. Consistent with this hypothesis, the proportion of $CD44^{high+}$ memory phenotype T-cells in the peripheral blood of mice that received B6 SPLs was much higher than that of wild-type (WT) B6 control mice during the observed period (Fig. 8A). In order to prevent homeostatic proliferation of mature T-cells, RAG2/gc-KO mice with BALB/c LSECs were immune reconstituted by BMT from B6 mice. RAG2/gc-KO mice that received B6 BMCs displayed similar levels of $CD44^{high+}$ memory T-cells and $CD45RB^{high+}/CD62L^{high+}$ naive T-cells to those in WT B6 control mice. The proportion of $NK1.1^+$ $CD3^-$ NK cells in the mice immune reconstituted using B6 BMCs fully resembled that in the WT B6 control mice, whereas the level in the mice immune reconstituted using B6 SPLs was markedly lower. In contrast, the

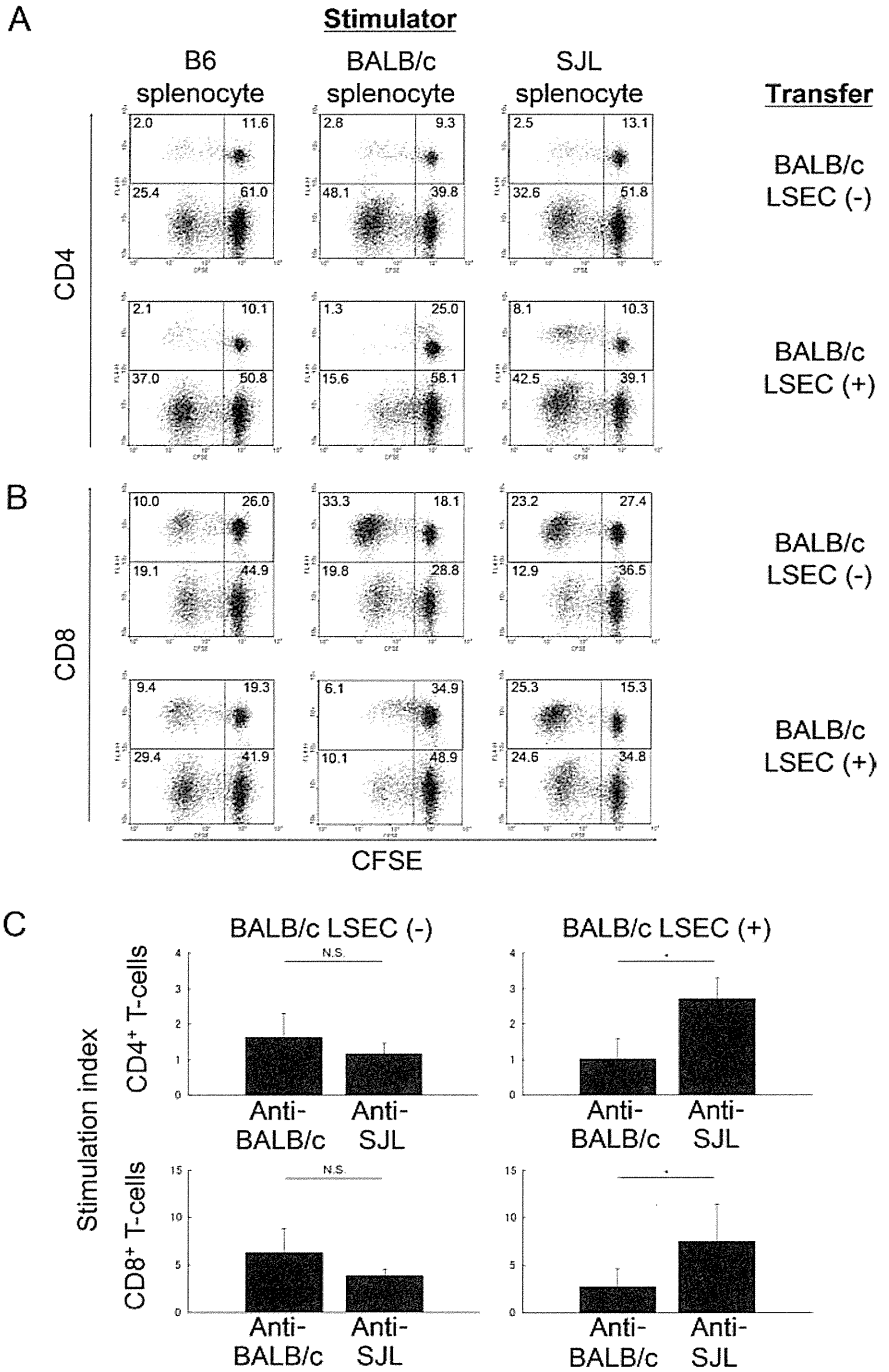

Figure 4. Allogeneic engraftment of the LSECs led to specific inhibition of T-cells responding to stimulation cognate with LSECs. RAG2/gc-KO mice were injected with BALB/c LSECs 2 days after MCT pretreatment. Six weeks after LSEC inoculation, B6 SPLs were injected into the recipient mice for immune reconstitution. One week after SPL inoculation, the recipient mice were sacrificed, and SPLs were obtained, carboxyfluorescein diacetate succinimidyl ester (CFSE) labeled, and cultured with stimulators. After 4.5 days of culture, the responder cells were analyzed by FCM. Using FCM analysis following mixed lymphocyte reaction (MLR), reactive T-cell proliferation can be visualized as the serial halving of CFSE intensity. (A, B) Representative FCM results of $CD4^+$ and $CD8^+$ T-cell division in the MLR using CFSE-labeled SPLs from the recipient RAG2/gc-KO mice as responders with irradiated SPLs from syngeneic B6 (left), allogeneic BALB/c (middle), or third-party SJL/j (right) mice as stimulators. The representative FCM profiles are shown ($n=4$ in each group). A total of 10,000 cells are shown in the FCM profile figure. The percentage value in total cells is shown in each quadrant. (C) Stimulation indices of $CD4^+$ and $CD8^+$ T-cells are shown. In the FCM analysis, $CD4^+$ and $CD8^+$ T-cells were gated and analyzed for CFSE fluorescence, and their stimulation indices were calculated. The average values of four independent mice in each group are shown. $*p<0.05$.

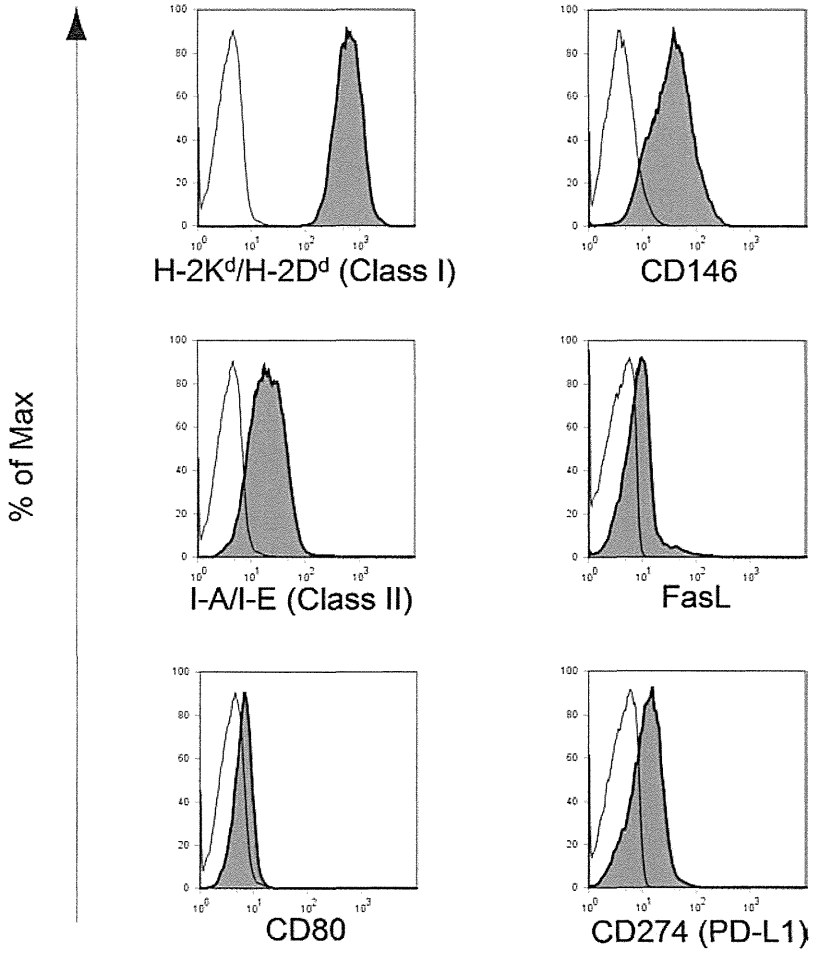

Figure 5. LSECs constitutively expressed Fas ligand (FasL) and programmed death ligand 1 (PD-L1), as well as molecules necessary for antigen presentation and CD146. The freshly isolated CD105$^+$ LSECs from BALB/c mice were stained for H-2K^d/H-2D^d (MHC-class I), I-A/I-E (MHC-class II), CD80, CD146 (another LSEC specific marker), FasL, and CD274 (PD-L1). These cells were analyzed by FCM. Dead cells were excluded from the analysis by forward scatter and propidium iodide. Thin and filled lines represent staining with isotype-matched control Abs and mAbs for the indicated surface molecule, respectively. The percent of Max is the number of cells in each bin of the histograms divided by the number of cells in the bin that contains the largest number of cells.

proportion of NK1.1$^+$ CD3$^+$ NKT-cells in the mice immune reconstituted using B6 BMCs did not markedly differ from that in the mice immune reconstituted using B6 SPLs (Fig. 8B).

Six weeks after BMT, there was no statistically significant difference in immune reconstitution levels (i.e., the proportion of CD4$^+$ and CD8$^+$ T-cells in the PBMCs) between recipient RAG2/gc-KO mice with allogeneic LSECs and corresponding control RAG2/gc-KO mice without allogeneic LSECs (Fig. 9A). When heart allografts from BALB/c mice were transplanted to recipients 6 weeks after BMT, heart survival in mice with allogeneic BALB/c LSEC engraftment was significantly prolonged compared with that in control mice without LSEC engraftment (Fig. 9B). On the other hand, survival of heart grafts from third-party SJL/j mice was not prolonged at all in mice with BALB/c LSEC engraftment (data not shown). These findings suggest that allogeneic LSECs can prolong the survival of subsequently grafted cognate allogeneic hearts.

DISCUSSION

LSECs have been described as a new type of APC that induces immune tolerance in naive T-cells (4,11,12,16). Following priming by antigen-presenting LSECs, CD4$^+$ T-cells fail to subsequently differentiate into the T helper 1 phenotype; instead, they differentiate into regulatory T-cells that express interleukin (IL)-4 and IL-10 upon restimulation (13,14). LSECs also have the capacity to present exogenous antigens on MHC class I molecules to CD8$^+$ T-cells, a process termed cross-presentation (16). Initially, stimulation of naive CD8$^+$ T-cells by LSECs results in

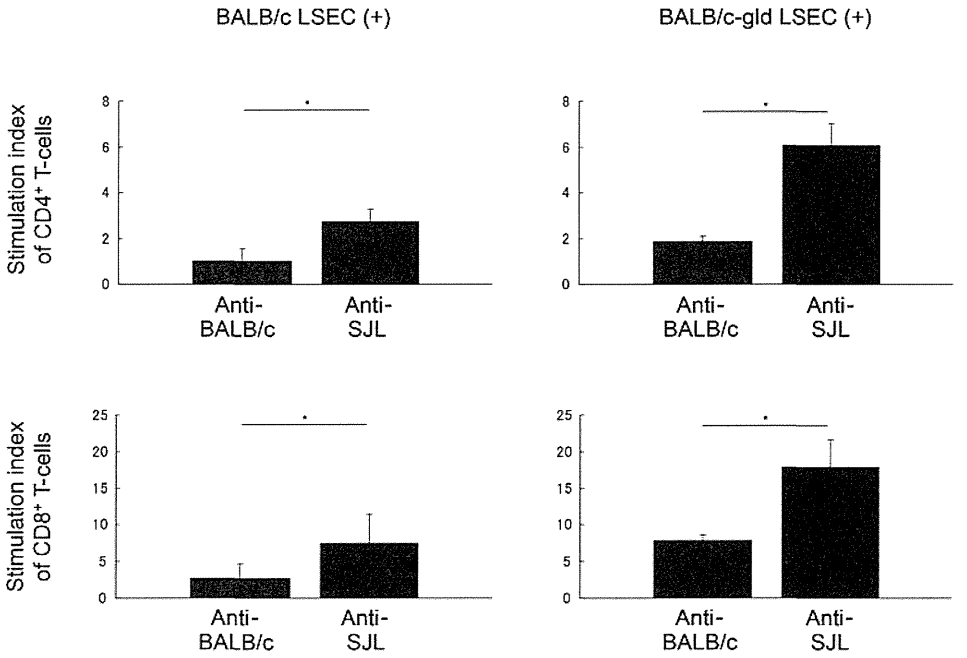

Figure 6. Engraftment with FasL-deficient LSECs did not attenuate the inhibitory effect of LSECs on alloreactive T-cells. RAG2/gc-KO mice were injected with BALB/c ($n=4$) or BALB/c-gld ($n=5$) LSECs 2 days after MCT pretreatment. Six weeks after LSEC inoculation, B6 SPLs were injected into the recipient mice for immune reconstitution. One week after SPL inoculation, the recipient mice were sacrificed, and the SPLs were obtained, CFSE labeled, and cultured with irradiated SPLs from syngeneic B6, allogeneic BALB/c, or third-party SJL/j mice as stimulators. After 4.5 days of culture, the responder cells were analyzed by FCM. Using FCM analysis following MLR, reactive T-cell proliferation can be visualized as the serial halving of CFSE intensity. In the FCM analysis, $CD4^+$ and $CD8^+$ T-cells were gated and analyzed for CFSE fluorescence, and their stimulation indices were calculated. The average values of four or five independent mice in each group are shown. $*p<0.05$.

T-cell proliferation and cytokine release. However, it ultimately leads to antigen-specific tolerance, as demonstrated by the simultaneous loss of cytokine expression and the failure of $CD8^+$ T-cells to develop into cytotoxic effector T-cells.

We previously demonstrated similar immunoregulatory effects of LSECs on T-cells with direct allospecificity beyond MHC barriers using an in vitro mixed LSEC-lymphocyte coculture model (23). In that model, cell–cell contact was necessary to induce the inhibitory effects of LSECs on alloreactive T-cell proliferation. In vivo, the cumulative surface area of LSECs is very large, and hepatic microcirculatory parameters allow frequent contact between LSECs and passenger leukocytes. Considering the large volume of blood that passes through the liver daily, it is probable that LSECs are ideally positioned within the liver to regulate alloimmune responses. By using this anatomical advantage of LSECs, we investigated the immunoregulatory effects of LSECs on alloreactive T-cells in an in vivo model in which exogenously inoculated allogeneic LSECs were engrafted orthotopically on the liver sinusoidal endothelium. MCT, which induces persistent cell cycle arrest through the G_2/M block in endothelial cells (24,29), was used in the present study to promote LSEC engraftment. MCT does not affect hepatocytes in this manner unless hepatic injury is redirected by additional drug toxicities or accumulation of toxic MCT intermediates through activation of cytochrome P450-induced metabolism MCT in hepatocytes (30). By this mechanism, MCT impairs only the host LSECs and confers a proliferative advantage to the transferred LSECs. Consistently, MCT administration significantly enhanced orthotopic engraftment of allogeneic LSECs (Fig. 1C). In this MCT-pretreated mouse model, allogeneic LSEC engraftment suppressed $CD4^+$ and $CD8^+$ T-cell proliferation in response to allostimulation by cells from mice cognate with LSEC donors.

The possible mechanisms for LSEC-induced suppressive immune regulation specifically on allogeneic T-cells might be associated with the death-inducing molecules that are constitutively expressed on LSECs (e.g., FasL, PD-L1). Morita et al. recently demonstrated the critical role of the PD-1/PD-L1 pathway in establishing immunological spontaneous tolerance status in mouse liver allografts (18). They found that PD-L1 was highly expressed on donor-derived tissue cells and is associated with infiltrating T-cell apoptosis in the allografts, and that blockade of this pathway leads to severe acute rejection.

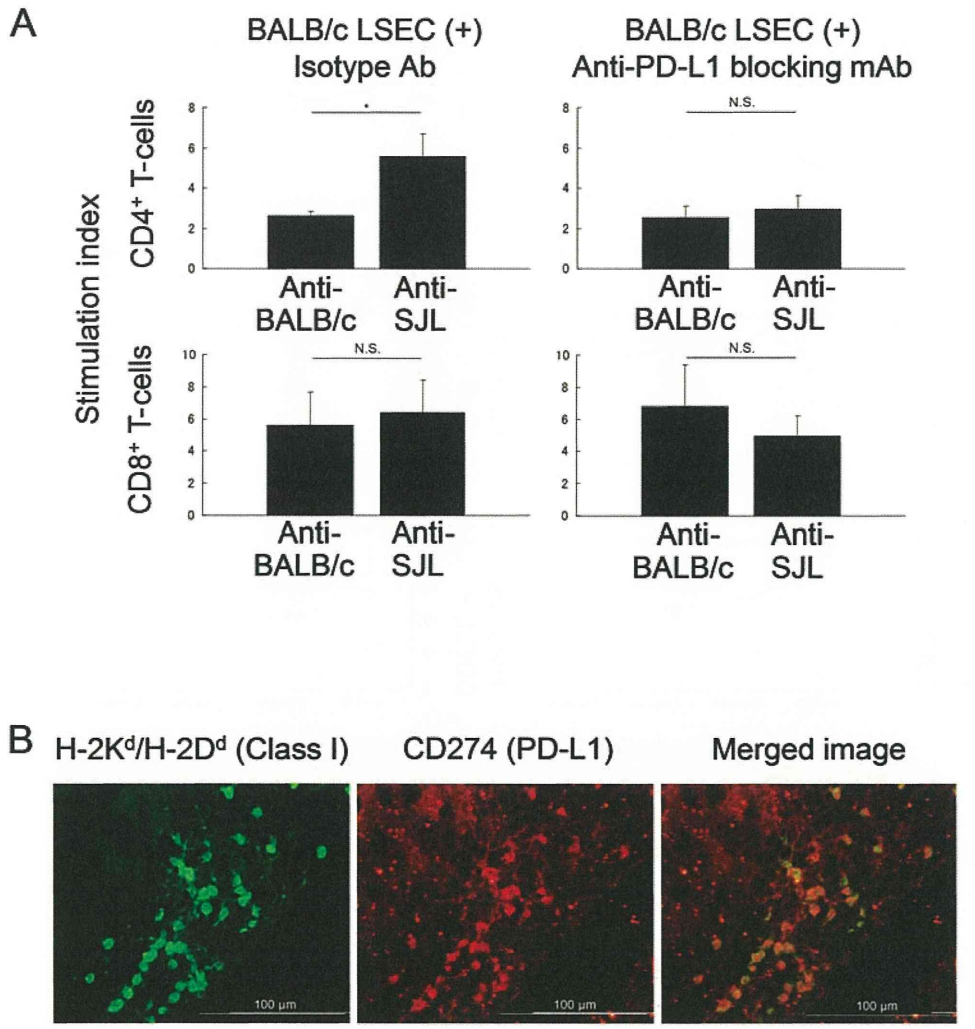

Figure 7. Administering anti-PD-L1 mAb during immune reconstitution attenuated the inhibitory effect of LSECs on alloreactive CD4+ T-cells. (A) RAG2/gc-KO mice were injected with BALB/c LSECs 2 days after MCT pretreatment. Six weeks after LSEC inoculation, B6 SPLs were injected into the recipient mice for immune reconstitution. To block PD-L1 signaling in vivo, the recipient mice were pretreated with 500 μg of anti-PD-L1 blocking mAb ($n=5$) or isotype-matched Ab ($n=3$) just before SPL inoculation. These antibodies were readministered 3 days later. One week after SPL inoculation, the recipient RAG2/gc-KO mice were sacrificed, and then the SPLs were isolated, CFSE-labeled, and cultured with irradiated SPLs from syngeneic B6, allogeneic BALB/c, or third-party SJL/j mice as stimulators. After 4.5 days of culture, the responder cells were analyzed by FCM. By using FCM analysis after the MLR, the reactive T-cell proliferation can be visualized as the serial halving of CFSE intensity. In the FCM analysis, $CD4^+$ and $CD8^+$ T-cells were gated and analyzed for CFSE fluorescence, and their stimulation indices were calculated. The average values of three or five independent mice in each group are shown. $*p<0.05$. (B) The engrafted LSECs persistently expressed PD-L1. RAG2/gc-KO mouse livers were obtained 7 weeks after LSEC inoculation and immunostained with FITC-conjugated anti-mouse $H\text{-}2K^d/H\text{-}2D^d$ (left) and anti-CD274-PE mAbs (middle) to estimate PD-L1 expression on the transferred LSECs. The right panel shows the merged image of the left and middle panels.

Although the cell type that contributes to PD-L1-induced negative regulation of T-cells in liver allografts remains to be identified, both their results and ours suggest that the signal between PD-1 on allogeneic T-cells and PD-L1 on LSECs likely inhibits corresponding T-cell function. The results of our previous in vitro study suggested that the Fas/FasL pathway also would be involved in LSEC-induced suppression of allogeneic T-cells (23). The lack of a significant role of FasL in LSECs could be explained by a limitation of allogeneic LSEC engraftment, since allogeneic LSECs have never replaced most native LSECs in an in vivo model. Alternatively, even when we used FasL KO mice as LSEC donors in the adoptive transfer to the allogeneic WT recipient mice, we could not rule out the

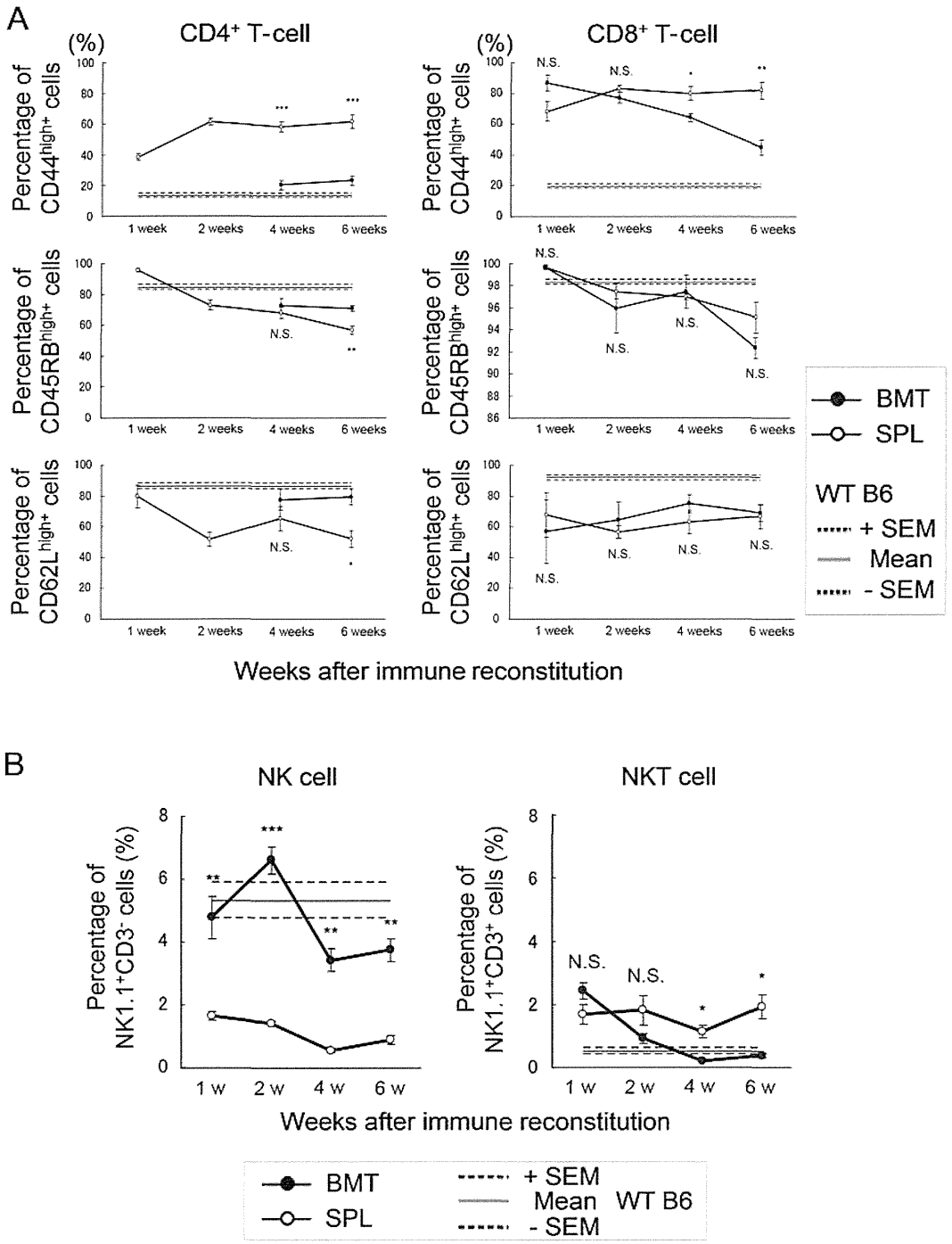

Figure 8. RAG2/gc-KO mice immune reconstituted with bone marrow cells (BMCs) showed a lower proportion of memory T-cells but a higher proportion of natural killer (NK) cells in their peripheral blood mononuclear cells (PBMCs) compared with the mice that were immune reconstituted with SPLs. B6 BMCs or SPLs were injected into RAG2/gc-KO mice through the tail vein. PBMCs from those RAG2/gc-KO or WT B6 control mice were analyzed by FCM. Anti-CD3, anti-CD4, anti-CD8, anti-CD44, anti-CD45RB, anti-CD62L, and anti-NK1.1 mAbs were used for surface staining of the PBMCs. (A) The proportions of $CD44^{high}$ memory phenotype, $CD45RB^{high}$, and $CD62L^{high}$ naive phenotype cells among each $CD4^+$ and $CD8^+$ T-cell fraction were determined after bone marrow transplantation (BMT) (filled circles) or SPL inoculation (open circles). The reconstituted $CD4^+$ T-cells began to be detectable 4 weeks after BMT. (B) The proportions of $NK1.1^+$ $CD3^-$ NK and $NK1.1^+$ $CD3^+$ NKT-cells among the PBMCs were determined after BMT (filled circles) or SPL inoculation (open circles). The mean values ± SEM of four independent mice in each group are shown. WT B6 mice were used as controls. The thin line indicates the mean and the dotted line indicates the SEM ($n=4$). $^*p<0.05$, $^{**}p<0.01$, $^{***}p<0.001$.

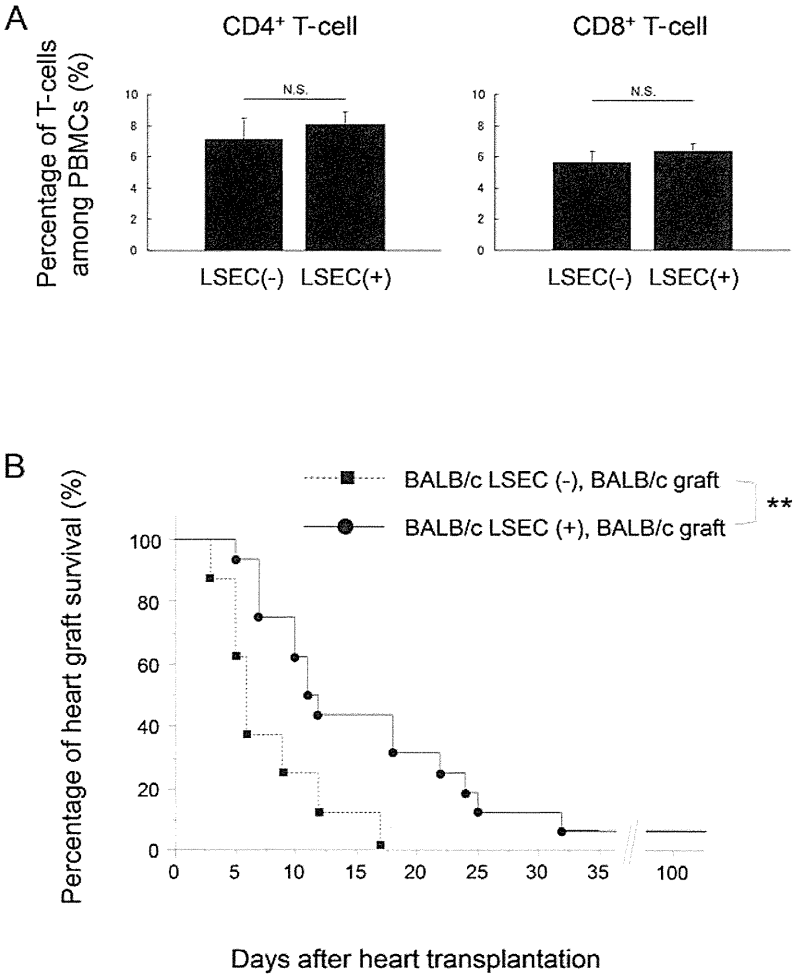

Figure 9. Transfer of allogeneic LSECs through the portal vein leads to prolonged survival of subsequently transplanted donor-type heart allografts in recipient mice immune reconstituted by BMT. (A) RAG2/gc-KO mice were reconstituted by B6 BMT. The RAG2/gc-KO mice were injected with BALB/c LSECs 2 days after the MCT pretreatment. Two weeks after the LSEC inoculation, B6 BMCs were injected into the recipient mice for immune reconstitution. Six weeks after BMT, PBMCs were obtained from the recipient mice, and the immune reconstitution level was evaluated by FCM. Anti-CD4 and anti-CD8 mAbs were used for the PBMC surface staining. In the FCM analyses, the percentages of $CD4^+$ or $CD8^+$ T-cells among PBMCs were measured in immune reconstituted RAG2/gc-KO mice with ($n=8$) or without ($n=6$) allogeneic LSEC inoculation. The frequencies of each indicated population among total number of obtained cells are shown. (B) Heterotopic heart transplantation after immune reconstitution by BMT in recipient RAG2/gc-KO mice with or without allogeneic BALB/c LSECs transfer. Heart allografts from BALB/c mice were subsequently transplanted into the recipient mice 6 weeks after BMT. Heart graft survival curves are shown. There is a significant difference ($^{**}p<0.01$) in heart allograft survival between recipient RAG2/gc-KO mice with (solid line, $n=16$) or without (dotted line, $n=8$) allogeneic LSEC transfer.

possibility of bidirectional transfer of MHC class II molecules between the WT recipient LSECs and the FasL-mutant donor LSECs after their inoculation. On the basis of the previous demonstration that T-cells can be positive for both donor and recipient MHC class II by intercellular transfer of MHC molecules and play a significant role in the antigen presentation (3), it is possible that recipient LSECs expressing FasL acquire donor MHC molecules, which might complicate the interpretation of this study. In contrast, when we used antibodies blocking PD-L1, they were able to block PD-L1 on both the donor and recipient LSECs, even if MHC transfer occurred. From such a standpoint, instead of the use of FasL KO mice, the use of anti-FasL-blocking mAb with/without anti-PD-L1-blocking mAb in the LSEC-chimeric mouse model might provide additional valuable information. Thus, to address the precise role of FasL and PD-L1 on LSECs in their inhibitory effects on alloreactive T-cells, further studies are required.

In addition to the death-inducing molecules, regulatory T-cells (Tregs) might also play a role in LSEC-induced suppression of allogeneic T-cells. It has been demonstrated

that LSECs prime CD4+ T-cells to a CD45RB^{low} memory phenotype lacking marker cytokine production for effector cells, and that those T-cells functionally belong to the CD25^{low} FoxP3^{-} Tregs (forkhead box P3 negative regulatory T-cell) family (15). Those LSEC-primed Tregs are thought to contribute to shifting antigen-dependent immune responses to tolerance toward exogenous antigens or endogenous self-antigens. A similar mechanism might be involved in the immunosuppressive effects of LSECs toward the alloreactive T-cells observed in the present study.

Engraftment of allogeneic LSECs prolonged the survival of subsequently grafted cognate allogeneic hearts in RAG2/gc-KO mice that were immune reconstituted by BMT (Fig. 9B) but not in RAG2/gc-KO mice that were immune reconstituted using SPLs. This difference could be explained by the homeostatic proliferation of inoculated splenic T-cells, which might lead to insusceptibility of those T-cells to LSEC-induced suppression. It has been reported that lymphopenia induces rapid expansion of T-cells, conversion from a naive to a memory-like phenotype, and development of effector functions (8,17). This phenomenon is thought to have an adverse effect on organ allograft tolerance induction in mouse models (19,31). An alternative explanation might be the insufficiency of either NK or NKT cells that have the capacity to release immunoregulatory cytokines, such as IL-10, in mice immune reconstituted with syngeneic SPLs. NK cells were supplied in the mice that were immune reconstituted by BMT (Fig. 8B) and might provide factors that induce the immunosuppressive features of the LSECs. It has been reported that host NK cells destroyed graft-derived APCs in a skin allograft model (33). In the absence of NK cells, donor APCs can survive and then migrate to host lymphoid and extralymphoid sites, where they directly stimulate the activation of alloreactive T-cells. T-cells activated in the absence of NK cells are possibly more resistant to LSEC-induced immunosuppression, and under such conditions, the prolongation of heart allograft survival might be difficult to achieve.

Nevertheless, only T-cells with direct allospecificity (i.e., those that recognize alloantigens via the direct pathway) would be suppressed by direct exposure to orthotopically engrafted allogeneic LSECs; T-cells with indirect allospecificity would theoretically not be influenced in the present in vivo model. This could be why most of the allogeneic hearts were eventually rejected even in LSEC-chimeric mice immune reconstituted by BMT, in contrast to the in vitro MLR assay results. Further studies are required to confirm this hypothesis.

In conclusion, allogeneic LSECs are capable of suppressing T-cells with specificity cognate to the LSECs in an in vivo murine model. The PD-1/PD-L1 pathway is likely involved in these suppressive effects.

ACKNOWLEDGMENTS: This work was supported by Grants-in-Aid for Young Scientists (Start-up) (2189015500) from the Japan Society for the Promotion of Science. The authors declare no conflict of interest.

REFERENCES

1. Benseler, V.; McCaughan, G. W.; Schlitt, H. J.; Bishop, G. A.; Bowen, D. G.; Bertolino, P. The liver: A special case in transplantation tolerance. Semin. Liver Dis. 27:194–213; 2007.
2. Benten, D.; Follenzi, A.; Bhargava, K. K.; Kumaran, V.; Palestro, C. J.; Gupta, S. Hepatic targeting of transplanted liver sinusoidal endothelial cells in intact mice. Hepatology 42:140–148; 2005.
3. Brown, K.; Sacks, S. H.; Wong, W. Extensive and bidirectional transfer of major histocompatibility complex class II molecules between donor and recipient T-cells in vivo following solid organ transplantation. FASEB J. 22:3776–3784; 2008.
4. Crispe, I. N. Hepatic T-cells and liver tolerance. Nat. Rev. Immunol. 3:51–62; 2003.
5. Crispe, I. N. The liver as a lymphoid organ. Annu. Rev. Immunol. 27:147–163; 2009.
6. Crispe, I. N.; Dao, T.; Klugewitz, K.; Mehal, W. Z.; Metz, D. P. The liver as a site of T-cell apoptosis: Graveyard, or killing field? Immunol. Rev. 174:47–62; 2000.
7. Follenzi, A.; Benten, D.; Novikoff, P.; Faulkner, L.; Raut, S.; Gupta, S. Transplanted endothelial cells repopulate the liver endothelium and correct the phenotype of hemophilia A mice. J. Clin. Invest. 118:935–945; 2008.
8. Gudmundsdottir, H.; Turka, L. A. A closer look at homeostatic proliferation of CD4+ T-cells: Costimulatory requirements and role in memory formation. J. Immunol. 167: 3699–3707; 2001.
9. Henriques-Pons, A.; Olivieri, B. P.; Oliveira, G. M.; Daeron, M.; de Araujo-Jorge, T. C. Experimental infection with *Trypanosoma cruzi* increases the population of CD8+, but not CD4+, immunoglobulin G Fc receptor-positive T lymphocytes. Infect. Immun. 73:5048–5052; 2005.
10. Knolle, P. A.; Gerken, G. Local control of the immune response in the liver. Immunol. Rev. 174:21–34; 2000.
11. Knolle, P. A.; Germann, T.; Treichel, U.; Uhrig, A.; Schmitt, E.; Hegenbarth, S.; Lohse, A. W.; Gerken, G. Endotoxin down-regulates T-cell activation by antigen-presenting liver sinusoidal endothelial cells. J. Immunol. 162:1401–1407; 1999.
12. Knolle, P. A.; Limmer, A. Neighborhood politics: The immunoregulatory function of organ-resident liver endothelial cells. Trends Immunol. 22:432–437; 2001.
13. Knolle, P. A.; Schmitt, E.; Jin, S.; Germann, T.; Duchmann, R.; Hegenbarth, S.; Gerken, G.; Lohse, A. W. Induction of cytokine production in naive CD4+ T-cells by antigen-presenting murine liver sinusoidal endothelial cells but failure to induce differentiation toward Th1 cells. Gastroenterology 116:1428–1440; 1999.
14. Knolle, P. A.; Uhrig, A.; Hegenbarth, S.; Loser, E.; Schmitt, E.; Gerken, G.; Lohse, A. W. IL-10 down-regulates T-cell activation by antigen-presenting liver sinusoidal endothelial cells through decreased antigen uptake via the mannose receptor and lowered surface expression of accessory molecules. Clin. Exp. Immunol. 114:427–433; 1998.
15. Kruse, N.; Neumann, K.; Schrage, A.; Derkow, K.; Schott, E.; Erben, U.; Kuhl, A.; Loddenkemper, C.; Zeitz, M.; Hamann, A.; Klugewitz, K. Priming of CD4+ T-cells by liver sinusoidal endothelial cells induces CD25^{low} forkhead

box protein 3- regulatory T-cells suppressing autoimmune hepatitis. Hepatology 50:1904–1913; 2009.
16. Limmer, A.; Ohl, J.; Kurts, C.; Ljunggren, H. G.; Reiss, Y.; Groettrup, M.; Momburg, F.; Arnold, B.; Knolle, P. A. Efficient presentation of exogenous antigen by liver endothelial cells to CD8+ T-cells results in antigen-specific T-cell tolerance. Nat. Med. 6:1348–1354; 2000.
17. Min, B.; Yamane, H.; Hu-Li, J.; Paul, W. E. Spontaneous and homeostatic proliferation of CD4 T-cells are regulated by different mechanisms. J. Immunol. 174:6039–6044; 2005.
18. Morita, M.; Fujino, M.; Jiang, G.; Kitazawa, Y.; Xie, L.; Azuma, M.; Yagita, H.; Nagao, S.; Sugioka, A.; Kurosawa, Y.; Takahara, S.; Fung, J.; Qian, S.; Lu, L.; Li, X. K. PD-1/B7-H1 interaction contribute to the spontaneous acceptance of mouse liver allograft. Am. J. Transplant. 10:40–46; 2010.
19. Moxham, V. F.; Karegli, J.; Phillips, R. E.; Brown, K. L.; Tapmeier, T. T.; Hangartner, R.; Sacks, S. H.; Wong, W. Homeostatic proliferation of lymphocytes results in augmented memory-like function and accelerated allograft rejection. J. Immunol. 180:3910–3918; 2008.
20. Ohdan, H.; Yang, Y. G.; Shimizu, A.; Swenson, K. G.; Sykes, M. Mixed chimerism induced without lethal conditioning prevents T-cell- and anti-Galα 1,3Gal-mediated graft rejection. J. Clin. Invest. 104:281–290; 1999.
21. Onoe, T.; Ohdan, H.; Ochi, M.; Tanaka, Y.; Tokita, D.; Hara, H.; Mizunuma, K.; Zhou, W.; Tashiro, H.; Asahara, T. Multiparameter flow cytometric mixed lymphocyte reaction assay using fluorescent cytoplasmic dye for assessing phenotypic property of T-cells responding to allogeneic stimulation. Transplant. Proc. 35:557–558; 2003.
22. Onoe, T.; Ohdan, H.; Tokita, D.; Hara, H.; Tanaka, Y.; Ishiyama, K.; Asahara, T. Liver sinusoidal endothelial cells have a capacity for inducing nonresponsiveness of T-cells across major histocompatibility complex barriers. Transpl. Int. 18:206–214; 2005.
23. Onoe, T.; Ohdan, H.; Tokita, D.; Shishida, M.; Tanaka, Y.; Hara, H.; Zhou, W.; Ishiyama, K.; Mitsuta, H.; Ide, K.; Asahara, T. Liver sinusoidal endothelial cells tolerize T-cells across MHC barriers in mice. J. Immunol. 175:139–146; 2005.
24. Shah, M.; Patel, K.; Sehgal, P. B. Monocrotaline pyrrole-induced endothelial cell megalocytosis involves a Golgi blockade mechanism. Am. J. Physiol. Cell Physiol. 288: C850–862; 2005.
25. Shishida, M.; Ohdan, H.; Onoe, T.; Tanaka, Y.; Igarashi, Y.; Banshodani, M.; Asahara, T. Role of invariant natural killer T-cells in liver sinusoidal endothelial cell-induced immunosuppression among T-cells with indirect allospecificity. Transplantation 85:1060–1064; 2008.
26. Suzuki, J.; Ricordi, C.; Chen, Z. Immune tolerance induction by integrating innate and adaptive immune regulators. Cell Transplant. 19:253–268; 2010.
27. Theuerkauf, I.; Zhou, H.; Fischer, H. P. Immunohistochemical patterns of human liver sinusoids under different conditions of pathologic perfusion. Virchows Arch. 438:498–504; 2001.
28. Tokita, D.; Shishida, M.; Ohdan, H.; Onoe, T.; Hara, H.; Tanaka, Y.; Ishiyama, K.; Mitsuta, H.; Ide, K.; Arihiro, K.; Asahara, T. Liver sinusoidal endothelial cells that endocytose allogeneic cells suppress T-cells with indirect allospecificity. J. Immunol. 177:3615–3624; 2006.
29. Wilson, D. W.; Lame, M. W.; Dunston, S. K.; Segall, H. J. DNA damage cell checkpoint activities are altered in monocrotaline pyrrole-induced cell cycle arrest in human pulmonary artery endothelial cells. Toxicol. Appl. Pharmacol. 166:69–80; 2000.
30. Wu, Y. M.; Joseph, B.; Berishvili, E.; Kumaran, V.; Gupta, S. Hepatocyte transplantation and drug-induced perturbations in liver cell compartments. Hepatology 47:279–287; 2008.
31. Wu, Z.; Bensinger, S. J.; Zhang, J.; Chen, C.; Yuan, X.; Huang, X.; Markmann, J. F.; Kassaee, A.; Rosengard, B. R.; Hancock, W. W.; Sayegh, M. H.; Turka, L. A. Homeostatic proliferation is a barrier to transplantation tolerance. Nat. Med. 10:87–92; 2004.
32. Xu, J.; Wang, D.; Zhang, C.; Song, J.; Liang, T.; Jin, W.; Kim, Y. C.; Wang, S. M.; Hou, G. Alternatively expressed genes identified in the CD4+ T-cells of allograft rejection mice. Cell Transplant. 20:333–350; 2011.
33. Yu, G.; Xu, X.; Vu, M. D.; Kilpatrick, E. D.; Li, X. C. NK cells promote transplant tolerance by killing donor antigen-presenting cells. J. Exp. Med. 203:1851–1858; 2006.

Conditional ablation of HMGB1 in mice reveals its protective function against endotoxemia and bacterial infection

Hideyuki Yanai[a,b,1], Atsushi Matsuda[a,1], Jianbo An[a], Ryuji Koshiba[a], Junko Nishio[a,b], Hideo Negishi[a,b], Hiroaki Ikushima[a], Takashi Onoe[c], Hideki Ohdan[c], Nobuaki Yoshida[d], and Tadatsugu Taniguchi[a,b,2]

[a]Department of Molecular Immunology, Institute of Industrial Science, University of Tokyo, Meguro-ku, Tokyo 153-8505, Japan; [b]Core Research for Evolution Science and Technology, Japan Science and Technology Agency, Chiyoda-ku, Tokyo 102-0075, Japan; [c]Department of Surgery, Division of Frontier Medical Science, Graduate School of Biomedical Sciences, Hiroshima University, Minami-ku, Hiroshima 734-8551, Japan; and [d]Laboratory of Developmental Genetics, Center for Experimental Medicine and Systems Biology, Institute of Medical Science, University of Tokyo, Minato-ku, Tokyo 108-8639, Japan

Contributed by Tadatsugu Taniguchi, November 5, 2013 (sent for review November 2, 2013)

High-mobility group box 1 (HMGB1) is a DNA-binding protein abundantly expressed in the nucleus that has gained much attention for its regulation of immunity and inflammation. Despite this, whether and how HMGB1 contributes to protective and/or pathological responses in vivo is unclear. In this study, we constructed *Hmgb1*-floxed (*Hmgb1*$^{f/f}$) mice to achieve the conditional inactivation of the gene in a cell- and tissue-specific manner by crossing these mice with an appropriate *Cre* recombinase transgenic strain. Interestingly, although mice with HMGB1 ablation in myeloid cells apparently develop normally, they are more sensitive to endotoxin shock compared with control mice, which is accompanied by massive macrophage cell death. Furthermore, these mice also show an increased sensitivity to *Listeria monocytogenes* infection. We also provide evidence that the loss of HMGB1 in macrophages results in the suppression of autophagy, which is commonly induced by lipopolysaccharide stimulation or *L. monocytogenes* infection. Thus, intracellular HMGB1 contributes to the protection of mice from endotoxemia and bacterial infection by mediating autophagy in macrophages. These newly generated HMGB1 conditional knockout mice will serve a useful tool with which to study further the in vivo role of this protein in various pathological conditions.

LPS | IL-1β | IL-18

Of the four members of the high-mobility group box (HMGB) family, HMGB1 is the best studied, given its versatile functions in various aspects of cellular responses (1–5). Ubiquitously expressed in all cells, HMGB1 is found en masse in the nucleus and is supposedly released into the extracellular fluid through an endoplasmic reticulum–Golgi pathway-independent mechanism from immune cells such as monocytes or macrophages after stimulation with lipopolysaccharide (LPS), proinflammatory cytokines, or nitric oxide (1, 6). The release of HMGB1 is also regulated by the inflammasome, a multiprotein oligomer that activates caspase-1 to promote the maturation of inflammatory cytokines, interleukin-1β (IL-1β) and IL-18, and by dying cells, typically those undergoing necrosis (7–10). Secreted or released, HMGB1 is known to participate in the activation of cell surface innate immune receptors, typically Toll-like receptors (TLRs), thereby affecting many aspects of the host's inflammatory responses upon infection or noxious stresses (1–5). Perhaps most notably is the crucial role of HMGB1 in LPS-induced endotoxemia, whereby administration of an anti-HMGB1 antibody significantly protects mice from lethality (1, 11). The study of released HMGB1 is complicated by a number of complex posttranslational modifications made to the protein, including acetylation and redox modifications that may regulate HMGB1 function (12–14).

HMGB1 can regulate immune reactions in several ways. Cytosolic HMGB1, together with the other members of the family, function as universal sentinels or chaperones for immunogenic nucleic acids by facilitating the recognition of nucleic acids by more discriminative, nucleic acid-sensing innate receptors (15–17). In addition, HMGB1 regulates autophagy, a cellular response that functions in clearing long-lived proteins and dysfunctional organelles to generate substrates for adenosine triphosphate (ATP) production during periods of starvation and other types of cellular stress events (13, 18–20). This mechanism contributes to antimicrobial responses against invading microorganisms (21, 22). Indeed, microorganisms can induce autophagy by stimulating innate immune receptors, such as TLRs, by a process in which bacteria are captured by phagocytosis but remain within intact vacuoles, an autophagic process termed microtubule-associated protein light chain 3 (LC3)-associated phagocytosis (LAP), which promotes the maturation of autophagosomes into autolysosomes (23, 24).

Collectively, these studies place HMGB1 in the center of immunological events where it uniquely functions intracellularly and extracellularly as a mediator of immune and inflammatory responses. The biological and clinical importance of HMGB1 is underscored by the dysregulation of this protein in a number of pathological conditions, including sepsis, ischemia–reperfusion injury, arthritis, and cancer (1, 3–5). Nonetheless, in vivo validation of the versatile functions described above is lacking due to the lethality of the *Hmgb1*-deficient mice, thought to cause lethal hypoglycemia in newborn mice (25). In the present study, we describe the generation of *Hmgb1*-floxed (*Hmgb1*$^{f/f}$) mice that

Significance

The high-mobility group box 1 (HMGB1) protein is abundantly expressed in the nucleus where it regulates chromatin function. More recently, it was found to also function in the cytoplasm and extracellular milieu for the regulation of immunity and inflammation. However, the in vivo study of HMGB1 has been hampered by the fact that HMGB1-deficient mice die soon after birth. In this study, we successfully generated *Hmgb1*-floxed mice to achieve conditional inactivation of the gene in a cell- and tissue-specific manner. We demonstrate that cytosolic HMGB1 in myeloid cells is critical for the protection of the host from endotoxemia and bacterial infection by inducing autophagy, a cellular response critical for maintaining cellular viability in the setting of various stresses including infection.

Author contributions: H.Y., A.M., and T.T. designed research; H.Y., A.M., J.A., R.K., and T.O. performed research; R.K. and N.Y. contributed new reagents/analytic tools; H.Y., A.M., J.A., J.N., H.N., H.I., T.O., and H.O. analyzed data; and H.Y. and T.T. wrote the paper.

The authors declare no conflict of interest.

[1]H.Y. and A.M. contributed equally to this work.

[2]To whom correspondence should be addressed. E-mail: tada@m.u-tokyo.ac.jp.

This article contains supporting information online at www.pnas.org/lookup/suppl/doi:10.1073/pnas.1320808110/-/DCSupplemental.

enabled the cell- and tissue-specific deletion of the gene when crossed with an appropriate *Cre* recombinase transgenic strain. We demonstrate in this study a protective role of intracellular HMGB1 in macrophages where it serves as a crucial regulator of autophagosome formation in the context of LPS stimulation or bacterial infection in vivo. Finally, we will discuss the future prospects of HMGB1 research using these newly generated mutant mice.

Results

Generation of *Hmgb1*$^{f/f}$ Mice. To study the function of HMGB1 in distinct cells and tissues, we generated mice with a conditional knockout of the *Hmgb1* gene by using the Cre-loxP system. As depicted in Fig. S1*A*, the targeting vector was constructed to cause the deletion of exons 2–4 upon expression of Cre protein. A neomycin resistance (*neo*) gene flanked by two loxP sites was introduced into intron 1 of the gene, whereas a third loxP site was generated downstream of exon 4. Mouse embryonic stem cells (ES) were electroporated with this vector, selected in the presence of G418 and then homologous recombinant clones identified by PCR and confirmed by Southern blot analysis (Fig. S1*B*). Cre protein was then transiently expressed in the targeted ES clones to delete the loxP-flanked *neo* gene (Fig. S1*C*). The resulting ES clones, carrying the loxP-flanked (floxed) *Hmgb1* gene, were used to generate chimeric mice that successfully transmitted the gene in the germ line. Mice homozygous for the floxed *Hmgb1* gene (*Hmgb1*$^{f/f}$) were born at the expected Mendelian ratios and presented with no obvious abnormalities. When these mice were crossed with mice transgenic for a CAG promoter-driven *cre* gene in which *cre* recombinase expression is constitutively and broadly driven by the cytomegalovirus early enhancer element and chicken β-actin promoter (26), mice died soon after birth, which is consistent with a previous report (25) (Fig. S2).

Ablation of the *Hmgb1* Gene in Myeloid Cells. In cells of myeloid lineage, in particular macrophages, HMGB1 is released following stimulation by TLR ligands or other noxious agents (1, 6), supporting the concept that HMGB1 plays a role in inflammatory responses. To examine the function of HMGB1 in these cells, we crossed *Hmgb1*$^{f/f}$ mice and mice with the *cre* gene inserted into the endogenous *M lysozyme* (*LysM*) locus. Mice carrying *Hmgb1*$^{f/f}$ and the *LysM cre* (*LysM*$^{Cre/+}$-*Hmgb1*$^{f/f}$) were born and developed normally. As shown in Fig. 1*A*, HMGB1 expression was barely detectable in peritoneal macrophages of these mice, whereas HMGB1 was expressed normally in other cells such as T and B lymphocytes (Fig. S3*A*). We further examined myeloid cell populations in the peritoneal cavity, spleen, blood, and bone marrow of these mice. As shown in Fig. 1*B*, no overt difference was found in the cellularity of the myeloid lineage, indicating that the loss of HMGB1 does not affect the development of these cells. Further, we observed no difference in the in vitro differentiation of M1 or M2 macrophages in *LysM*$^{Cre/+}$-*Hmgb1*$^{f/f}$ mice (Fig. S3*B*).

Susceptibility of *LysM*$^{Cre/+}$-*Hmgb1*$^{f/f}$ Mice to LPS-Induced Endotoxemia. There has been a particular focus on HMGB1 in the context of LPS-induced endotoxemia, wherein HMGB1 released by myeloid cells is reported to be capable of activating various innate receptors, especially TLR4, and thereby exacerbating pathogenic inflammatory responses (11, 27). We therefore first examined whether and how *LysM*$^{Cre/+}$-*Hmgb1*$^{f/f}$ mice respond to LPS. We observed that *LysM*$^{Cre/+}$-*Hmgb1*$^{f/f}$ mice were more vulnerable to i.p. injection of LPS and were accompanied by a massive amount of tissue destruction in the lungs compared with *LysM*$^{+/+}$-*Hmgb1*$^{f/f}$ mice (Fig. 2*A*). This observation indicates there is a protective role of HMGB1, which seemingly contrasts with the prevailing notion that it exacerbates endotoxemia (1, 2, 11).

We then examined serum levels of proinflammatory cytokines thought to participate in the pathogenic response to LPS and found that levels of TNF-α, IL-6, and IL-12p40 in *LysM*$^{Cre/+}$-*Hmgb1*$^{f/f}$ mice were similar to those found in *LysM*$^{+/+}$-*Hmgb1*$^{f/f}$ mice (Fig. 2*B*). Interestingly, however, there was a notable increase of IL-1β and IL-18 in the serum of the *LysM*$^{Cre/+}$-*Hmgb1*$^{f/f}$ mice, indicating a hyperactivation of an inflammasome pathway(s) (Fig. 2*C*). In this experimental setting, serum HMGB1 levels were only marginally lower compared with those of *LysM*$^{+/+}$-*Hmgb1*$^{f/f}$ mice (Fig. 2*D*), demonstrating that myeloid cells are not the main source of LPS-induced serum HMGB1 and that the increased vulnerability to LPS reflects a function of intracellular HMGB1 vis-à-vis extracellular HMGB1.

The elevated IL-1β and IL-18 expression in the serum of the LPS-stimulated *LysM*$^{Cre/+}$-*Hmgb1*$^{f/f}$ mice prompted us to examine the activation of the inflammasome in the mutant macrophages. We stimulated macrophages from *LysM*$^{Cre/+}$-*Hmgb1*$^{f/f}$ mice with LPS and ATP and then examined IL-1β and IL-18

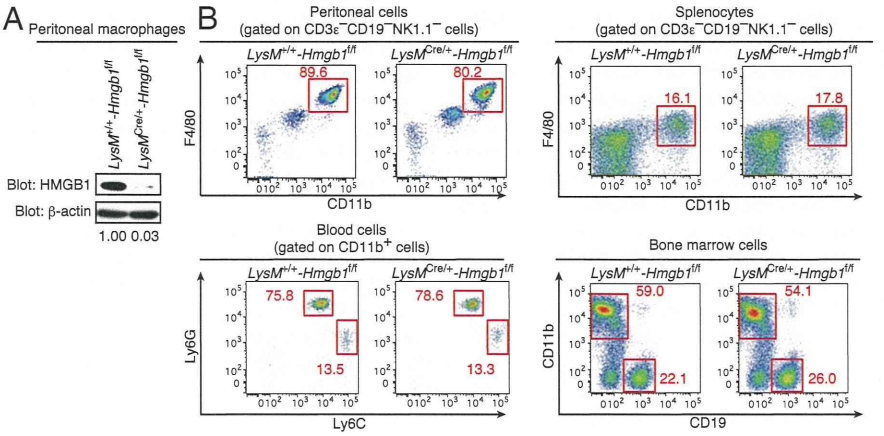

Fig. 1. HMGB1 expression and myeloid cell population of *LysM*$^{Cre/+}$-*Hmgb1*$^{f/f}$ mice. (*A*) Peritoneal macrophages were obtained from *LysM*$^{+/+}$-*Hmgb1*$^{f/f}$ and *LysM*$^{Cre/+}$-*Hmgb1*$^{f/f}$ mice. Whole cell extracts (20 μg) were prepared and subjected to immunoblot analysis to detect HMGB1 protein. HMGB1 band density is presented relative to β-actin band density. (*B*) Single cell suspensions were prepared from the peritoneal cavity, spleen, peripheral blood, and bone marrow from *LysM*$^{+/+}$-*Hmgb1*$^{f/f}$ or *LysM*$^{Cre/+}$-*Hmgb1*$^{f/f}$ mice and stained with the indicated combination of the following fluorochrome-conjugated antibodies: anti-F4/80 PerCP-Cy5, anti-CD11b APC, anti-Ly6G PE-Cy7, anti-Ly6C FITC, anti-CD19 PB, anti-NK1.1 PB, and anti-CD3ε PB antibodies. CD3ε$^-$CD19$^-$NK1.1$^-$ cells (*Upper*) or CD11b$^+$ cells (*Lower Left*) were gated and shown. The numbers represent the percentage of cells contained in each region.